

- gun/turret performance
- control optimization techniques for achieving high inertial stabilization
- effect of sensor locations on the servo controllers
- synthesis concepts for the selection of all-electric drive system components
- system structural design concepts of all-electric drive systems
- synthesis concepts for the gun/turret servo systems. The material presented is based on the accumulated experience of Elbit in past company projects, performed for a number of customers world-wide.

The paper covers the following topics:

This paper details with the synthesis, design concept and methodology of all-electric high power gun/turret drive servo systems. The material presented is based on the accumulated experience of Elbit in past company projects, performed for a number of customers world-wide.

## ABSTRACT

Davidov Gavriel, D.Sc., ELBIT Computers Ltd.  
Combat Vehicle Systems Division

**SELECTED TOPICS ON THE SYNTHESIS AND ANALYSIS OF ALL-ELECTRIC HEAVY GUN/TURRET DRIVE CONTROL SYSTEMS**

- These topics are described as basic elements in the construction of combat systems with two main objectives:
  - To achieve a highly accurate inertial positioning of the gun, even in the presence of major ground velocity disturbances.
  - To enable the gunner to drive the system in very low velocities despite friction, imbalance and ground disturbances.

The main goal of a gun/turret combat system is to achieve a high first-shot hit probability in all combat conditions, such as, static and on the move. It enables the crew to "hit first before being hit", thus destroying the enemy and at the same time survive. To achieve this purpose, the following requirements are essential: a rigid mechanical structure, effective gun/turret stabilizer and fire control, high mobility and low velocity and at the same time survivability.

Most of the drives of today's Main Battle Tanks (MBT) are hydraulic drives. However, in the course of the last decade, a new trend is being introduced, to integrate electric drives in tanks. For example, the Israeli MBT Merkava Mark 3 is the first tank serially manufactured, whose turret is driven by an all-electric drive system. The drive is produced by Elbit Systems Ltd., the British MRII, the German M1, the Japanese MBT Types 74 & 90 and the Soviet MBT T-80U, equipped with an electric drive in the traverse axis only.

Most of the drives of today's Main Battle Tanks (MBT) are hydraulic drives. However, in the course of the last decade, a new trend is being introduced, to integrate electric drives in tanks. For example, the Israeli MBT Merkava Mark 3 is the first tank serially manufactured, whose turret is driven by an all-electric drive system. The drive is produced by Elbit Systems Ltd., the British MRII, the German M1, the Japanese MBT Types 74 & 90 and the Soviet MBT T-80U, equipped with an electric drive in the traverse axis only.

The main goal of a gun/turret combat system is to achieve a high first-shot hit probability in all combat conditions, such as, static and on the move. It enables the crew to "hit first before being hit", thus destroying the enemy and at the same time survivability. To achieve this purpose, the following requirements are essential: a rigid mechanical structure, effective gun/turret stabilizer and fire control, high mobility and low velocity and at the same time survivability.

With an MBT mission profile, the operational load on the electrical drive system during a typical fighting day can be defined. In addition to the required electrical power, the gear drive rigidity and the heat profile of the motors can be estimated. Following main issues: mission profile, environmental conditions and ground disturbances.

Selection of the drive components must take into consideration the consumption. From the control point of view, the electric drive has a better linearity dynamic, higher mechanical stiffness, higher efficiency of consumption. From the control point of view, the electric drive has a work in very low temperature conditions and a lower energy maintenance free service, considerably quieter operation, longer life.

Moreover, the electric drive enables faster installation, longer higher crew safety due to elimination of flammable hydraulic oil.

The main advantages of all-electric drives over hydraulic drives are, selection of the drive components must take into consideration the consumption. From the control point of view, the electric drive has a better linearity dynamic, higher mechanical stiffness, higher efficiency of consumption. From the control point of view, the electric drive has a work in very low temperature conditions and a lower energy maintenance free service, considerably quieter operation, longer life.

Motors. Tests. The system is developed by Delco Electronics Division of General MB770/XM803 version, with speeds of up to 40km/hr, in cross-country traverse. These results have been measured in the US - German milliradian (one sigma) in elevation and 0.4 milliradian (one sigma) in servo controllers), can achieve a gun stabilization accuracy of 0.2 milliradian (one sigma) in addition, "director-type systems" which include a stabilized two axes gunner's mirror (which slaves the gun inertial position via sigma). In addition, "director-type systems" which include a stabilized stabilization error from 1 to 0.5 milliradian (with probability of one output of these gyros is utilized to improve the gun stabilization accuracy. Ogorokiewicz reports that such control strategy improves the include two additional feed forward gyros. One traverse gyro is mounted in the hull. The second elevation gyro is mounted in the turret. The in the paper of Ogorokiewicz [2], the second generation tank stabilizers accuracy. Ogorokiewicz reports that such control strategy improves the output of these gyros is utilized to improve the gun stabilization the T-72.

addition to difficulties with the gun aiming function in low velocities in gyro technology and to the hydraulic drive system limitations. This, in a limited stabilization performance due to the limitations of the Soviet elevation control loop of the gun. The control configuration in T-72 has the T-72.

A more complex control structure can be found in the Soviet T-72 tank [3]. It comprises two rate gyros and one rate integrating (R.I.) gyro, mounted on the gun.

This set of requirements from a servo control system, yields the required sensors for stabilization and the control functions for effective gun regulation. A basic conventional control methodology [1,2] yields two rate gyros mounted on the gun in order to achieve inertial stabilization. For example, such system control can be found in the American MBT M60. However, such a control scheme leads to a limited performance. This, due to the non-linearity of the mechanical hydraulic system and the limited quality of the gyros.

Information on ground disturbances will enable to define the structural requirements of the servo control system. Such information will also enable to define the stabilizer attenuator function, in order to achieve the desired gun stabilization accuracy.

With available data on the environmental conditions in which the system will have to operate, the extreme temperatures, shocks and vibrations ranges can be defined.

- In this paper it is shown that the same and even better stabilization accuracy can be achieved without the need to resort to two axes with an all-electric drive system whose stabilizer includes the basic two stabilized mirrors. Such accuracy can be achieved in an MBT equipped gun inertial servos and the additional two feed forward gyros only.
- A new advance in MBT servo control systems can be found in the French tank Leclerc named "Sivier" [4], which is manufactured by SFI M. It includes a Central Sensor Block (CSB) mounted in the turret. Elevation gun stabilization is achieved by enslaving a relative gun control loop to the CSB. Turret stabilization is achieved by using the CSB inertial sensors.
- Beyer et al. [5] suggested in their patent to include a CSB, or strap down and/or gyros in the turret. The gun stabilization is achieved in two stages. First by closing relative control servo loops. The relative loops are based on relative sensors (angle pick-up, tachometers and/or resolvers). Second, the loops track inertial commands from the CSB.
- Such a scheme has the following advantages:
- a) The CSB is located in a protected position.
  - b) An arbitrary number of devices may be simultaneously stabilized.
  - c) When a CSB includes 3 gyros and 3 accelerometers, it can be utilized for navigation missions.
  - d) Gun stabilization accuracy depends on the quality of the relative sensors (tachometers, resolvers, shaft encoder), on backlash value of the trunion axis.
  - e) A higher velocity accuracy range of the CSB gyros is needed, compared to the gyros mounted on the stabilized gun. This, in consequence, stabilizes the gun inertial dynamics.
  - f) In order to achieve high gun inertial position accuracy, additional feed forward sensors are required, besides the CSB (hull gyro, inertial inclinometer). Such a configuration is extremely expensive.

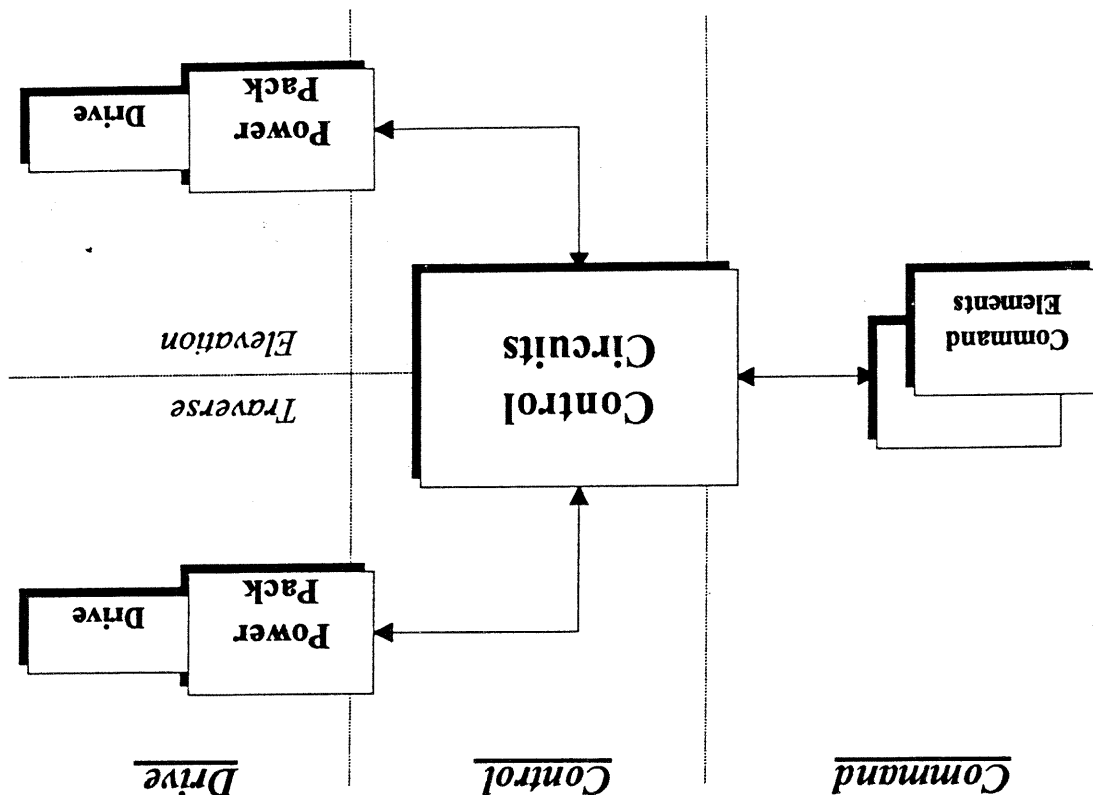
Main limitations of the CSB are:

- a) The CSB is located in a protected position.
- b) An arbitrary number of devices may be simultaneously stabilized.
- c) When a CSB includes 3 gyros and 3 accelerometers, it can be utilized for navigation missions.
- d) Gun stabilization accuracy depends on the quality of the relative sensors (tachometers, resolvers, shaft encoder), on backlash value of the trunion axis.
- e) A higher velocity accuracy range of the CSB gyros is needed, compared to the gyros mounted on the stabilized gun. This, in consequence, stabilizes the gun inertial dynamics.
- f) In order to achieve high gun inertial position accuracy, additional feed forward sensors are required, besides the CSB (hull gyro, inertial inclinometer). Such a configuration is extremely expensive.

A non-classical servo control MBTs stabilizer is suggested in Scheib [6]. He proposed a sophisticated adaptive control for an all-electric, Large Turret Drive System (LDS). The control technique is based on a Lyapunov direct method. Simulation results reveal good stabilization performance. However, no experimental results are reported.

In this paper, a new insight on topics related to the construction of all electric drive systems for MBT is given. The paper is organized as follows: In Chapter two, a description of general all-electric drive system structures is given. In Chapter three, a methodology for the selection of basic electrical drive parameters is given, based on customer requirements. In Chapter four, dynamic models of an all electrical turret drive are described. With such models, a simulation program for an electric drive is constructed. In Chapter five, optimization control techniques for achieving high stabilization accuracy are described. Conclusions are given in Chapter six.

Figure 2.1: Gun and Turret Drive System - Basic Structure



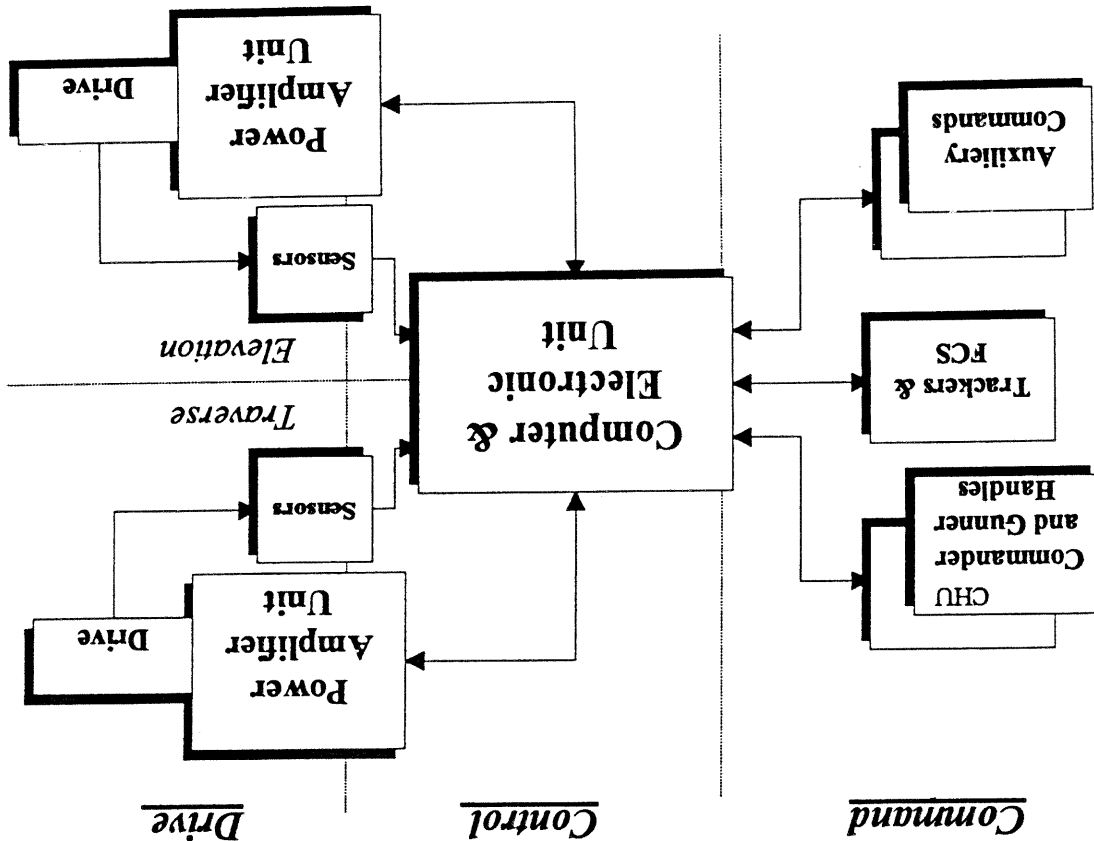
However, the performance of today's modern GTDS systems is incomparable to these, previous generation versions. This, in view of their advanced system configuration, as well as, the fundamental technological progress achieved in all domains comprising the GTDS, including sensors, drive technology and electronics.

The basic biaxial drive structure was established approximately 60 years ago with the development and publication of the first Gun and Turret Drive Systems (GTDSs), in their European or American versions. This structure (see Figure 2.1), with some modifications, remains valid and unchanged to this day, even for the latest and most advanced versions.

## 2.1. GENERAL

### 2. ALL ELECTRIC DRIVE SYSTEM - STRUCTURE

Figure 2.2 : GTDS - Basic Configuration



Modern GTDS configurations include some derivatives of the basic structure in order to satisfy new requirements, such as, high quality stabilization, high precision in spatial positioning, high velocity and acceleration, increased safety etc. The configuration responding to these new requirements is presented in Fig. 2.2.

## 2.2. CONFIGURATIONS OF GUN & TURRET DRIVE SYSTEMS

A discussion of the present solutions and future trends, constitutes the main issue of the following paragraph.

As a result of this progress, a more detailed configuration, based on the same basic structure will be presented, including new trends and developments.

In this system configuration, the command section is presented in more details in order to describe the possible command sources. However, the most important difference, versus the basic structure, will be the separate blocks for traverse and elevation sensors which may include position, velocity (relative and inertial) and acceleration sensors. These sensors are tightly connected to the gun or the turret (represented by the drive block) and are fully controlled by the Computer and Electronic Unit (CEU).

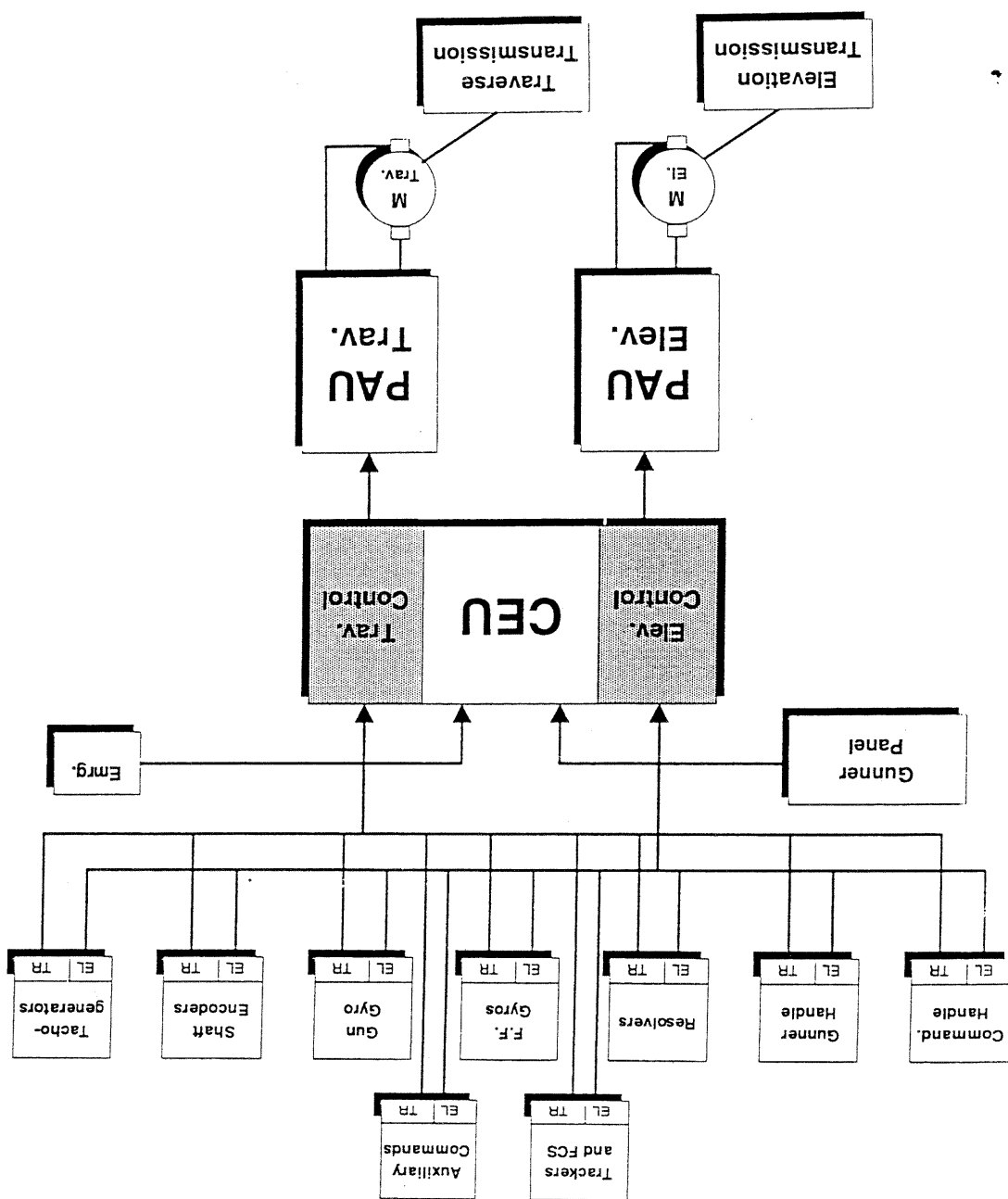
Given that the two control axes are theoretically orthogonal, the cross-correlation between the sensors of traverse and elevation is practically neglected. The outputs of those sensors, as well as the system if the less-than-ideal construction of the GTDS configuration, introducing some cross-coupling elements.

This independence and separation between the drive elements of each axis, resulted in the modification of the GTDS configuration, introducing separate drive and control channels as detailed in figure 2.3.

In this approach, the CEU is divided into three functional sub-units: two Control Blocks and the Common Block. The Common Block is responsible for all operational tasks, inter-channel calculations and corrections, parameter updates, BLT, etc.

The separate channel approach with a new structure of the CEU, simplifies the system implementation for better system availability and fault tolerance.

Figure 2.3 : GTDs - Modified Configuration



The new trends in GTDS constitute a direct response to the new MBT requirements. These include: improved survivability, greater fire power and full operability under extreme conditions. In light of these requirements, a new set of gun parameters was established, providing a new set of requirements for the GTDS.

The following are some examples of these new parameters and requirements:

- **Survivability**

The survivability requirement is covered by a large variety of solutions, especially heavy armor, which generally provides a turret with high inertia and an extremely high unbalance. These parameters imply a new strength, stiffness and power requirements for the GTDS and the turret bearing. On the other hand, the survivability calls for GTDS fault tolerance and system operability even after partial ballistic damage. In such a case, partial performance or performance degradation will be acceptable.

- **Fire Power**

Fire power requirements are a direct result of the modern battlefield analysis, including target and threat analysis. According to this scenario, fast and accurate turret gun jump between different types of targets becomes the most important parameter for fire power, as well as, for survivability. These parameters imply new requirements for acceleration, turret and gun positioning and sophisticated motion control.

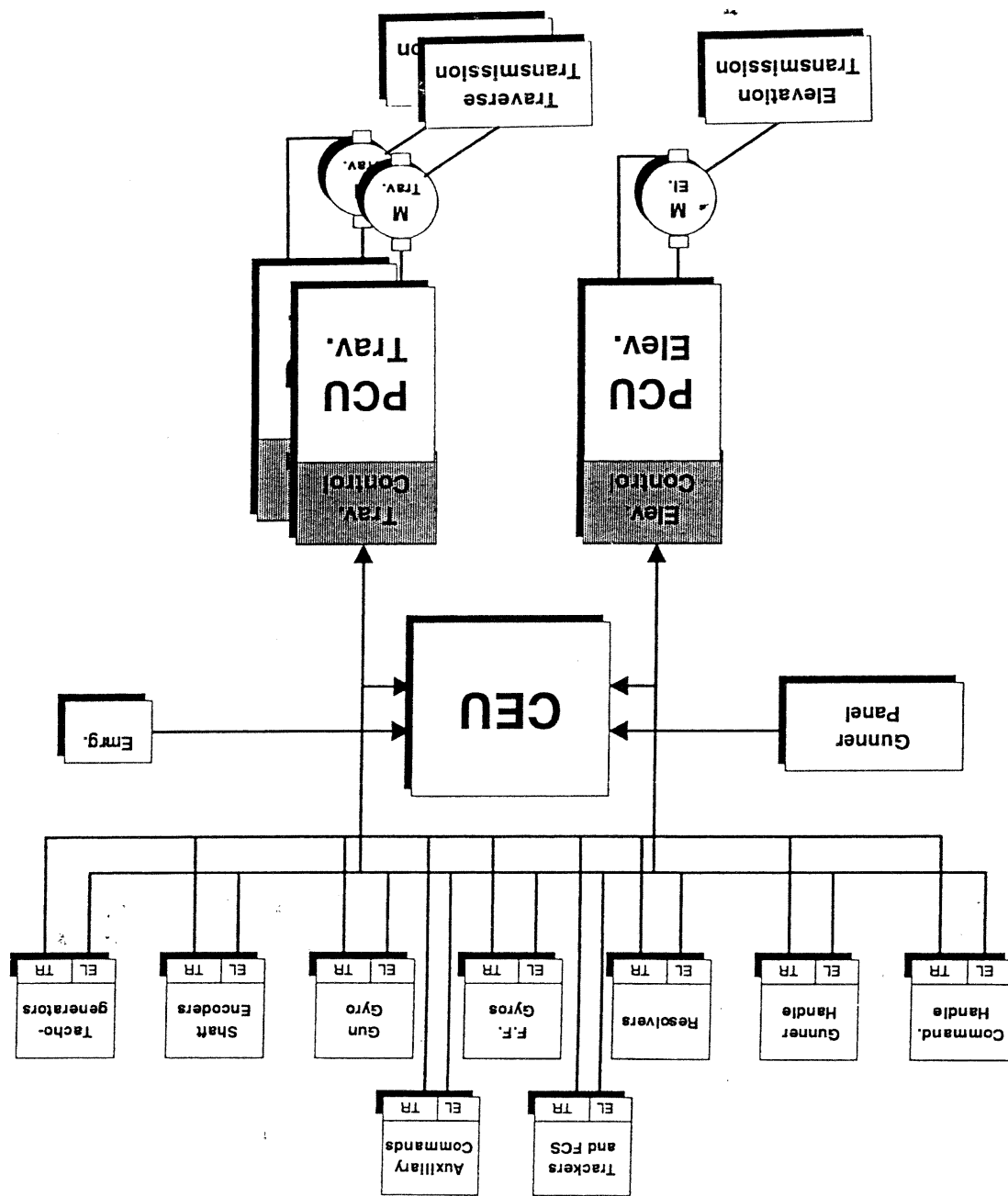
The above examples are the basic reason for the trend to implement the hydraulic solutions. The driving forces in this trend are, the survivability stabilization system (GTDS) type, instead of the conventional modern drive systems of the all Electrical Gun and Turret Drive & requirements. The GTDS system availability and safety of operation is achieved through a special system configuration, which takes into account the system partitioning and the installation concept.

The modern developments of all electric drive systems will utilize the approach of separate drive channels (as mentioned above), as an additional step toward system availability. The conjunction of Power electronics and motion control integrated Power and Control Unit (PCU), should simplify this issue. In this type of implementation, additional progress can be achieved by providing a fusion between the motion control and current control of the power stage of the PCU. Multiple drive channels, including per-channel-control, implement a distributed control system with full system redundancy. This type of system configuration is presented in Fig. 2.4.

Avoidance of high pressure, flammable hydraulic oil in the MBT, represents an additional and probably the most important parameter of the superiority of EGTDs, in comparison with the hydraulic turreted drive systems.

This configuration provides the most interesting solution for good system availability. This, due to a redundancy in traverse and the avoidance of singular critical functions.

**Figure 2.4: EGDS - Modem System Configuration**



(\*) 2<sup>o</sup> in APG course at speed of 20 kmh.

PARAMETER	TRAVEL	ELEVATION	ACCELERATION	AT 0 DEG.	AT 15 DEG.	ACCELERATION	AT 30 DEG.	IMBALANCE	MOENT OF INERTIA	STABILIZATION	ACCURACY (*)
MAX. VELOCITY	0.6÷0.8 Rad/sec	0.6÷0.8 Rad/sec	0.25 Rad/sec	0.5 Rad/sec	0.20 Rad/sec	0.00 Rad/sec		100÷1000 Nm	20000÷45000 Nm	4000÷600 Kg <sup>2</sup>	0.25 MRad
MIN. VELOCITY											
ACCELERATION											
AT 0 DEG.											
AT 15 DEG.											
ACCELERATION											
AT 30 DEG.											
IMBALANCE											
MOENT OF INERTIA											
STABILIZATION											
ACCURACY (*)											

TABLE 1: A List of Modern MBT Parameters

In Table 1, a list of modern MBT parameters and performance requirements are given. The listed parameters serve as a basis for deriving the drive parameters.

3.2. SYSTEM REQUIREMENTS

In this chapter, general performance requirements of Large Turret Drive Systems (LTDs), as well as, general mechanical parameters of an MBT turret are presented. The desired performance requirements serve as a basis for the selection of drive parameters. A framework for deriving basic drive parameters is described. It is followed by mathematical relations to the MBT required performance including drive torques, gear ratios, drive power etc.

### 3.1. GENERAL

### ALL ELECTRIC BASIC DRIVE COMPONENT SELECTION -

### METHODLOGY

Our experience indicates that gear ratio selection must be based on criteria, relevant to optimal LDS stabilization and to optimal transmission of torque, high power, velocities and acceleration from drive to large turret and gun loads.

This result is known as "inertia match".

Where:  $J_1$  is the load moment of inertia and  $J_2$  is the motor and gear moment of inertia.

(1)

$$N = \sqrt{\frac{J_1}{J_2}}$$

is:

In a case where no opposing torque acts on the load, the optimal value is found by minimizing the motor armature energy dissipation function. In literature [7], the optimal value of gear coupling ratio is determined. It

### 3.3.1. GEAR COUPLING RATIO SELECTION

In this chapter, a framework based on customer requirements for deriving basic drive parameters namely: gear coupling ratio, motor coefficients, drive torques and drive power, is given. Useful mathematical expressions for deriving basic parameters of the system, are analyzed and synthesized.

**3.3. SELECTION OF BASIC DRIVE PARAMETERS**

The desired maximum velocities and accelerations detailed in table 1, indicate the MBS's stabilizer performance for ground disturbance attenuation and for rapid gun/turret sector positioning. The minimal desired velocity indicates the aiming potential of the drive. The required acceleration in 15 deg and 30 deg indicates the drive's power to compete with the imbalance and friction load moments. The stabilization accuracy indicates the stabilizer performance and the time on target probability during tank on move. In the following chapters, an analysis and synthesis of the drive parameters based on the information detailed in table 1, is given.

The factor 0.15 is a consequence of stabilization requirement (see chapter 3).

Where:

$$N = \sqrt{J_m / J_d}$$

(5)

4. The ratio between drive inertia  $J_d$  and load inertia  $J_m$ , namely to load and  $J_d$ , is the load moment of inertia, respectively.  $T_m$ ,  $T_d$  are load's and motor & drive's Coulomb friction moments respectively,  $J_m$  is the motor & drive's moment inertia transmitted

Where:

$$N = \frac{T_m}{T_d} = \frac{(J_m + J_d) \alpha_m}{J_d + T_m}$$

(4)

3. The ratio between maximum load (gun/turret) due to acceleration  $T_m$ , and motor's peak torque  $T_m$ , namely

$$N = \frac{\omega_m}{\omega_m}$$

(3)

2. The ratio between maximum disturbance velocity at the hull  $\omega_m$  and maximum motor velocity  $\omega_m$ , namely

$$N = \frac{\omega_m}{\omega_m}$$

(2)

1. The ratio between gun minimum aiming velocity  $\omega_m$  and minimum motor velocity  $\omega_m$ , namely

The information listed in table 1 defines the gear drive ratio parameter  $N$ , whose calculation is based on the following equations:

acceleration.

a - Is the linear load inertia acceleration and  $g$  is the gravity

Where :

$$(8) \quad t_m > \frac{N}{T_f + T_g + T_w (1 \pm \frac{g}{a_{max}}) + a_{max} (J_1 + J_2)}$$

- c) Torque required for rated acceleration of loads and motors' inertia translated to load namely
- b) Static and dynamic load imbalance moment
- a) Motors, gear and load friction moments

2. During stabilization, the motor's rated torque  $t_{rated}$  must be higher than the sum of:

$$(7) \quad t_m > \frac{N}{T_w + T_f + T_g}$$

- 1. Motors' maximal moment  $t_m$  must be higher than the sum of the load imbalance moment  $T_w$ , load friction moment  $T_f$ , motors and gear friction moments  $T_g$  namely

The motor's moments can be evaluated by employing the information given in table 1 and the following relations:

### 3.3.2. MOTOR MOMENT AND COEFFICIENT SELECTION

The designer must find an optimum gear ratio  $N$  for each axis such that it satisfies the relations above.

$$(6) \quad N = \frac{t_m}{T_{w_{max}} \sin(\theta_{max}) + T_f + T_g}$$

- 5. The ratio between the maximal turret imbalance  $T_{w_{max}}$  at maximal cant angle  $\theta_{max}$  and motor's peak torque (for traverse axis) namely

Note that such equations are relevant for brush and brushless motors units.

The motors moment coefficient has the same value of  $K_e$  as the MKS

$$K_e = \frac{Q}{V_{line} - V_{dissipation} + N} \quad (11)$$

The motors velocity coefficient can be derived by employing the electric line voltage, gear ratio, electrical dissipation voltage and the desired maximum load angular velocity  $Q$ , namely

The above equations enable to estimate the drive's required moments.

$$t_m^{\text{peak}} > \frac{T_{line-u_0} * \sin(\alpha_{max}) + T_g + T_f + (J_m + J_i) * \alpha_{max}}{N} \quad (10)$$

- a) Gear-motor and load friction moments
  - b) Maximal acceleration moment of load and drive's inertia
  - c) Load imbalance moment for acceleration:
4. Traverse motor's peak moment  $t_m^{\text{peak}}$  must be greater than the sum of:

$$t_m^{\text{peak}} = \frac{T_{line-u_0} * \sin(\alpha_{max}) + T_g + T_f}{N} \quad (9)$$

- a) Turret imbalance moment, which depends on the sine of the cant angle
  - b) the turret and the gear-motor friction's moments namely
3. Traverse motor's permanent moment  $t_m^{\text{per}}$  must be greater or equal to the sum of :

Following selection of the basic drive parameters, it is convenient to supply extensive information on the desired drive. Detailed simulations enable the optimization of drive parameters and current and power can be employed during simulation runs. Such have to be merged with a detailed dynamic nonlinear model of a gun turret system (see chapter 3). Calculations of average and RMS drive measured or synthesized ground velocities and moment disturbances using dynamic simulation of the MBT's task profile. For this purpose, A complementary method is to estimate the effective drive power by The current is scaled for the operational voltage of the drive system. Information is translated to currents and velocities as a function of time. The mission profile contains several 50-80 minute cycles. This

define the drive's spectral characters such as natural frequencies, resonance and frequency bandwidth. For this purpose, dynamic drive models and a simulation system will be required. These are detailed in the following chapter.

STAGE NO.	ACTIVITY	DURATION
1.	Aiming Tank in Stabilization Mode	T1
2.	Driving and Vehicle Maneuvers	T2
3.	Vehicle Maneuver with High Slopes	T3
4.	Searching in Stabilization Mode	T4
5.	Pause	T5

TABLE 2: Example of a One Cycle Task Profile for an MBT

For estimation of the drive's power - a mission is required. Such a profile includes duration and a mix of operations during one combat day. An example for such a cycle is given in table 2.

### 3.3.3. DRIVE POWER SELECTION

Note that the tachometer measures the rotation of the motor shaft relative velocity while the gyro, connected to the bottom of the gun's breech block, measures the inertial elevation velocity of the gun. Both tachometer and gyro, measure velocity, from the tachometer output.

In fig 4.1, an example of the measured spectral transfer functions of a tachometer and a gyro, versus the electric motor current in the elevation axis of a MBT prototype is given.

A convenient approach to validate compatibility of the mathematical models to reality is, to use spectral techniques. With such techniques, the parameters of the simulated model are optimized such that the transfer functions of the measured and the simulated model, will be as similar as possible.

Compatibility with the reality, is not described in these reports. Lagrangian formulation. In [6] a dynamic model for an all electric drive derivation of the dynamic equation of motion is based on the a tank is given. However, the validation of such models and their for a tank is given. In [6] a dynamic model for an all electric drive

- a) Power amplifier current control model
- b) Drive's gear and motor models
- c) friction and backlash models
- d) gun/turret models

The methodology for selection of spectral and non-linear drive dynamics. The dynamic models are: models of the dynamic elements that construct the complete drive and time domain. The drive structure described in chapter 1, yields role in the optimization of drive performance parameters in frequency program of the drive system. This simulation program plays an essential role in the optimization of drive system. Such simulation of a system is analyzed. Such models are a basis for the construction of a simulation and turret dynamics. In this chapter dynamic models are described and parameters is based on mathematical models which describe the gun

## 4.1. GENERAL

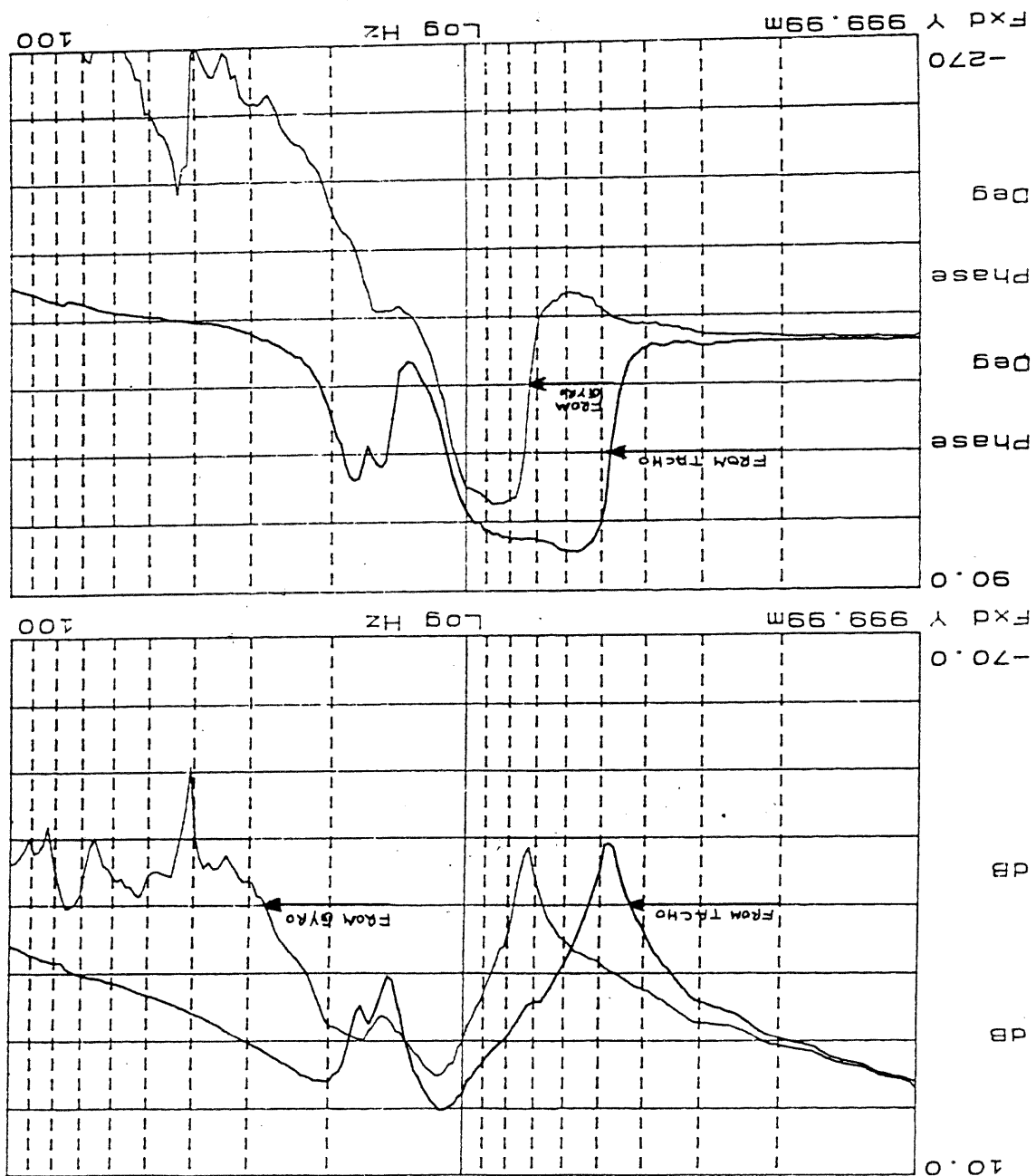
### 4. DRIVE DYNAMICS MODELS

The transfer function between the electric current of the motor (which is relative to the motor's moments and acceleration) and the measured velocity should be a pure integration. However, the measured transfer functions depicted in fig (4.1) indicate that only for low frequencies, they exhibit large differences in their behavior. Below 3 Hz, do both behave like integrators. For higher frequencies, they are developed in Elbit Ltd., can describe, with a high compatibility, the measured information.

In this chapter, it is shown that the above mentioned dynamic models, developed in Elbit Ltd., can describe the nonlinear parameter values. A detailed description of the dynamic models follows.

Moreover, the models' analytic functions are employed as a design tool. They are used to select the detailed drive's specific and nonlinear parameters. A detailed description of the dynamic models follows.

Figure 4.1: Tachometer and gyro versus current command -  
Bode diagram - as measured



$$I_m = \frac{1+sT_a}{1+T_a} I^o(s) \quad (16)$$

Eq. (15) indicates a proportional and a pure integrator controller (PI).

$I^o$  is the command current to the motor.

Where:

$$R(I^o - I_m) + \frac{L}{R^2} \int (I^o - I_m) dt = V \quad (15)$$

The equation of the current controller, according to Schreib [6] is:  
 value and  $T_a$  is an external moment which acts on the motor's shaft.  
 and velocity coefficients respectively,  $T_a$  is the motor's Coulomb friction  
 motors torque,  $\tau_m$  is the motor's velocity,  $K_v$ ,  $K_t$  are the motor's torque  
 $L$ ,  $R$  are the motor's induction and resistance respectively,  $T_a$  is the  
 where  $V$  is the input voltage to the motor,  $I_m$  is the current motor,

$$T_a = I_m K_t \quad (14)$$

$$J_m \frac{d\omega_m}{dt} = T_m - T_a - T_d \quad (13)$$

$$V_m = L \frac{di_m}{dt} + R * I_m + K_v * \omega_m \quad (12)$$

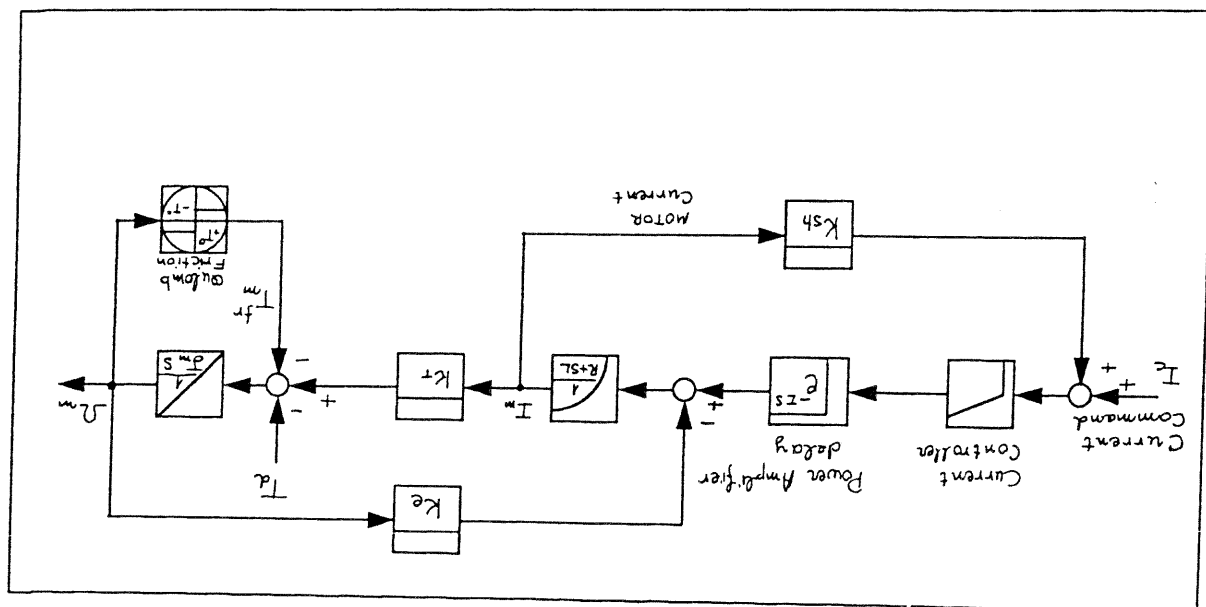
the following equations:  
 represented by a pure time delay. The motor dynamic is described by  
 From the control point of view, the power amplifier dynamics is

Wideband Modulation) amplifier.  
 in Figure 4.2. It features an electric motor controlled by a PWM (Pulse  
 The model's block diagram for the power amplifier and motor is shown

#### 4.2.1. POWER AMPLIFIER CURRENT LOOP MODEL

#### 4.2. MODELS

Figure 4.2: Power amplifier and DC motor - block diagram



In systems where closed tracking is not required, it would be sufficient to use current controllers that include only a PI controller, as described by Schieib [6]. When close tracking is required,  $G(s)$  must include at least two pure integrations (two PI controllers), one to compensate for the pure zero and the second to compensate for steady state errors of constant current commands. Not much was published on this, other than the work of Schieib [6], who extended and analyzed the problem of current controllers to include several pure integrators, theoretically and practically.

The back EMF is described as a disturbance to the current loop. Exact expression of the back EMF as a function of the moment of inertia of the load shows that the transmission function ( $I_m / V_m(s)$ ) has at least one pure zero. In low frequencies, when good tracking is required for constant speed, this produces a disturbance to the current loop that could interfere with good control of the motor.

$G(s)$  is the controllers transfer function,  $\zeta_m K_m$  is the back EMF. Where:

$$I_m = [(I^o - I_m) * G(s) - \zeta_m K_m] * \frac{S_L + R}{1} \quad (17)$$

If the back EMF is not ignored then the control equation is lead to limited performance, explained as follows.

However, our analysis indicates that Schieib's controller proposal may system sensitivity to changes in resistance and reluctance of the electric motor's pole. The current feedback allows the reduction of the control of the motor's current, moments and shaft acceleration. Also, for a wide range of frequencies,  $I_m \approx I^o$ , which offers a direct control of the motor's current, moments and shaft acceleration.

Schieib recommended to select  $\zeta_m = 0.1$ ,  $\tau_m = 0.1 * (L/R)$ , where  $\tau_m$  is the

and  $\Omega_1$ ,  $\Omega_2$  are the angular velocities of the motor and the load, respectively, and  $t_0$  denotes the time immediately before and after the impact between the gear's teeth. Kittiuch clarified, with the aid of simulations, the effects of changes in the restitutioon coefficient on the dynamics of the transmission.

$$e^x = \frac{U_m(t_1) - U_l(t_1)}{U_m(t_0) - U_l(t_0)} \quad (20)$$

and  $e^*$  is the restitution coefficient, defined by:

$$(19) \quad \frac{^1\zeta + ^m\zeta}{^1\zeta - ^m\zeta} = \zeta.$$

$$(18) \quad K^A = \frac{4K_A j}{\left[ \frac{\ln \left( \frac{e^x}{K} \right)^{-2}}{1 + \left( \frac{\ln \left( \frac{e^x}{K} \right)^{-2}}{2} \right)} \right]^{1/2}}$$

Kittich [8] shows that the relationship between  $K_x$  and  $K_y$  is:

[8]. Kiticch focused on gear transmissions, as shown in fig. 4.3, which relate the moment of the load and drive. A block diagram of a drive's gear with a backlash is given in fig. 4.4 with the following terminology:  $J_1$ , is the motor's and transmission's moment of inertia,  $J_2$ , is the load's moment of inertia,  $T_1$  and  $T_2$ , are the Coulomb friction moments of the motor/transmission and the load, respectively,  $K_x$ , is the rigidity of the transmission and the load, respectively,  $K_y$ , is the self-locking coefficient of the transmission and  $K_z$ , is the self-locking damping coefficient. It is obvious that the transmission is affected by the relative displacements between the load and those are translated into two principal moments. One of the moments is proportional to the relative angular displacement between the drive axis and the load, and the other moment is proportional to the relative rigidity of the transmission. The other moment is proportional to the relative angular displacement between the drive axis and the load, and the elastic damping of the transmission out at AEG by Kiticch

Figure 4.3: Gear drive (After KLITTCHE) - block diagram

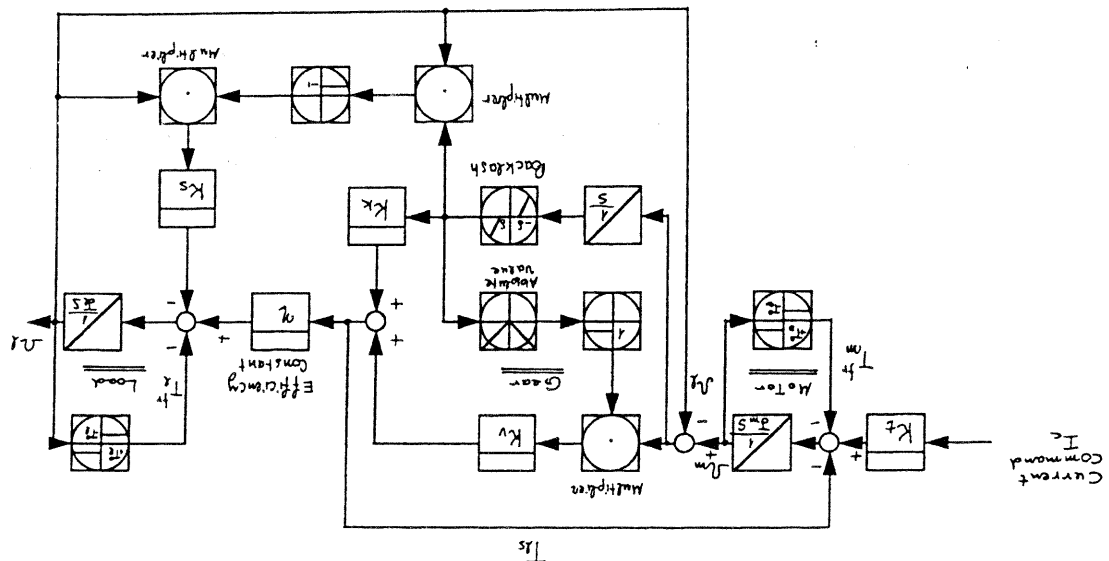


Figure 4.3: Gear description (After KLITTCHE)

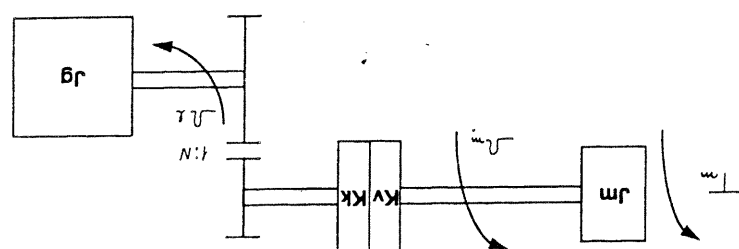
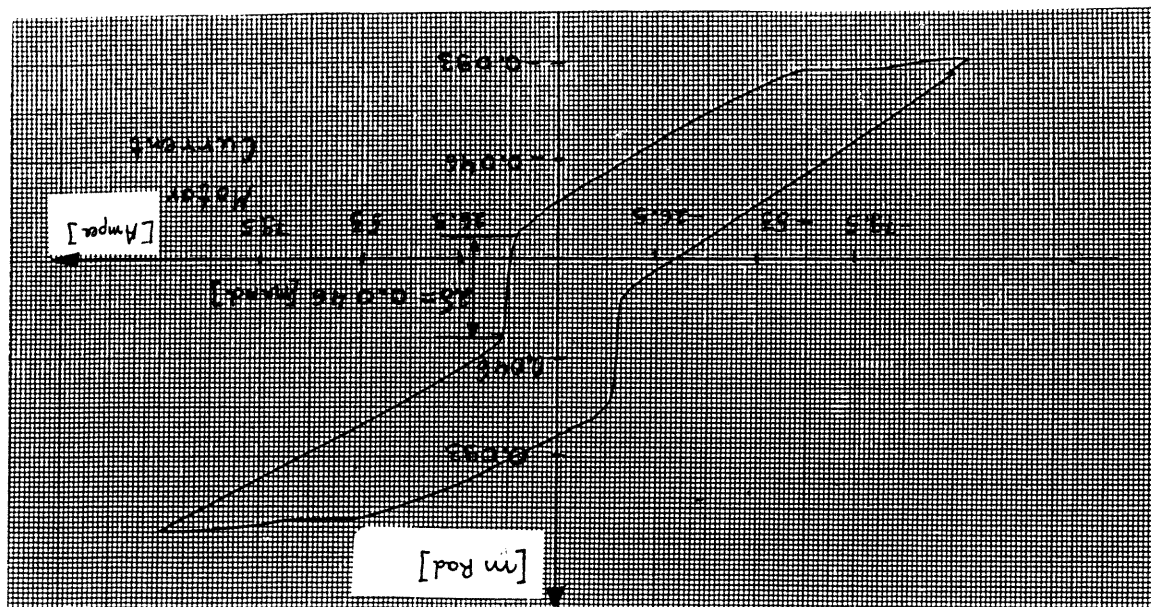


Figure 4.5: Hysteresis curve of a gear drive - as measured



However, our direct measurements of gears' hysteresis function, depicted in fig. (4.5), imply that a more elaborate gear model is needed to prevent resonance in transmissions. Such hysteresis function (a motor current versus motor shaft angle) is done by rotating slowly the motor shaft with a harmonic function while the load is stacked by an extremal lock. This measured information yields a nonlinear stiffness function of  $K_e$  (not given here for the sake of brevity).

When the restitution coefficient is one ( $e_r = 1, K_r = 0$ ) the response of the transmission is quite oscillatory and when the restitution coefficient is zero ( $e_r = 0, K_r = 2\sqrt{K_e}$ ), the damping is immediate. Obviously, it is important to select materials of low restitution coefficients in order to prevent resonance in transmissions.

The transmission is quite oscillatory and when the restitution coefficient is zero ( $e_r = 0, K_r = 2\sqrt{K_e}$ ), the damping is immediate. Obviously, it is important to select materials of low restitution coefficients in order to prevent resonance in transmissions.

The classical friction models used are described by static maps between velocity and friction force [8,9,10]. It is well known that friction causes problematic effects on the performance of servo control drive systems. The main concern is the non-linear dynamic model of the Coulomb friction. The traditional friction model is based on a significant system.

### Coulomb friction

Coulomb friction moment are described below. Implemented with minimal backlash. Models for the backlash and mechanisms. In any case, gear installations in an MBT must be therefore, it is recommended to construct the gears with anti-backlash sophisticated digital controller as discussed in chapter 4. However, the gear backlash phenomenon is much more difficult to compensate. High friction and imbalance moments can be compensated by a attractive system with high performance, our experience shows that plant with severe stability limitations. In order to achieve a cost the drive has low friction and high backlash, yields an uncontrollable excellent system performance but is very expensive. The case where the ideal case where the drive has low backlash and low friction, yields it is known that mechanical to minimize the backlash, yield high friction.

The drive's nonlinear effects, namely friction, imbalance moments and backlash, cause degradation and severe limitations of the system's performance. It can be shown that for small signals, the backlash and friction causes disconnection between motor moments and load, which means an open loop. Such open loop causes delays, oscillations, instability and an inability to achieve control of a bandwidth, the desired stabilization accuracy of 0.1 mil (one sigma).

### 4.2.3. DRIVE NON LINEAR MODELS

Our experiments' results show that the proposed model is adequate for friction model predicts essential non linearity. velocity slew rate. Both activities occur in low velocity which the affects both the MBT stabilizatior accuracy and the aimimg minimal our case. With such a dynamic model, it is realized that friction moment given [12].

The MBT elevation closed loop velocity axis is driven by a harmonic command is low. In literature, more complicated friction models are motor velocity. However, no movement occurs when the velocity appproximatively described by motor current, behaves as the sign of the velocity are shown. It is obvious that the friction moment, which is low velocity command. The velocity command, motor current and

This model indicates that when the absolute value of the static friction is higher than the sum of the external load moments, no moment acts on the load. However, if the sum value of extremal moments acting on the load, is higher than the sum of the extremal load moments, the load is driven by the net moment. In fig. 4.6 an experiment for measuring the friction force dynamics is depicted.

$\Sigma T$  - is the sum of all extremal moments acting on the load.  
 $T_0$  - is the absolute value of the Coulomb friction moment.

Where:

$$\left. \begin{array}{l} \Sigma T - T_0 * \text{sgn}(\Sigma T) \\ \|\Sigma T\| > T_0 \\ 0 \\ \|\Sigma T\| < T_0 \\ \Sigma T = 0 \\ T_0 * \text{sgn}(\Sigma T) \\ \|\Sigma T\| > 0 \end{array} \right\} \quad (21)$$

However the model is inaccurate for low velocities. We propose a more elaborate model described by the following equations:

It can be seen that backlash characteristic is a non differentiable non-linearity. It has been recognized as one of the factors severely limiting the performance of feedback systems.

$\alpha$  - is the velocity ground disturbance.  
 $\theta$  - is the backlash value.

Where:

$$T_B = \begin{cases} K_s * (\int (\alpha_s - \alpha_l - \theta) dt) + K_v * (\alpha_s - \alpha_l - \theta) & \theta \leq \theta \\ \int (\alpha_s - \alpha_l - \theta) dt & \theta > \theta \end{cases} \quad (22)$$

The gear backlash model is given in [8] and is described in fig. The equations of which, combined with the gears' internal moments are given as follows:

### Backlash

Figure 4.6: Dynamic torque of Coulomb friction - as measured

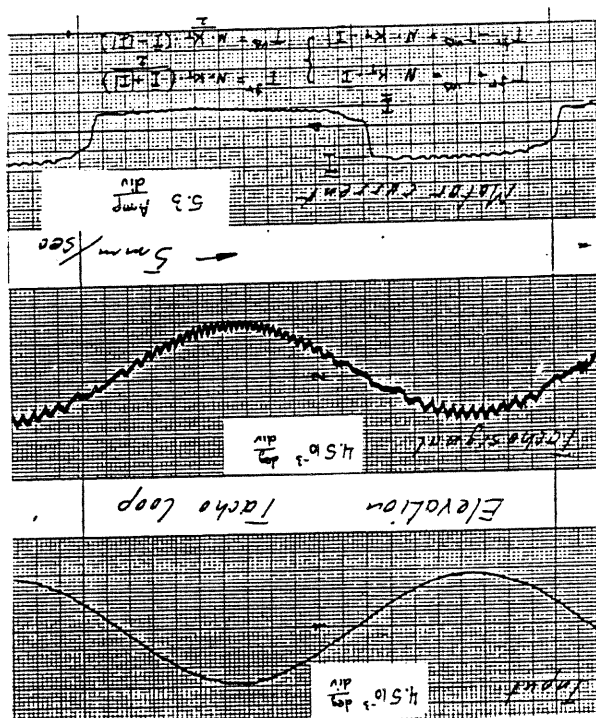


Fig 4.8 represents a complete block diagram of an all-electric drive system in the elevation axis. The traverse axis has a similar block diagram which is omitted here for the sake of brevity. A linear spectral analysis of the drive's block diagram transfer functions is given in the next paragraph.

(22 - 25) above. For the sake of brevity they are omitted here. Actually, the traverse model equations have the same form given in Eq.

(25)

$$J_1 = J_g + J_s$$

(24)

$$\frac{dQ}{dt} = T_{gear} - T_{drive} - T_s - T_l$$

(23)

$$T_s = (Q_s - Q_g) K_{s1} + K_{s2} \int (Q_s - Q_g) dt$$

(22)

$$\frac{dQ}{dt} = \frac{J_g}{T_s}$$

The gun/turret of a tank is modeled in fig. 4.7. In this model,  $J_1$ , is the moment of inertia of the breech block,  $J_g$ , is the moment of inertia of the gun barrel,  $T_s$  is the imbalance moment,  $K_{s1}$ ,  $K_{s2}$  are the spring and damping coefficients connecting the breech block and the barrel. The moment also depends on the difference in angles and angular velocities between the load (gun barrel) and the drive (motor). The mathematical equations describing this relationship are:

#### 4.2.4. GUN/TURRET MODEL

Asymmetry of the mass structure of the gun/turret relative to their rotational axes yields imbalance moments. Such moments are influenced by transitsional and gravitational accelerations. This may oppose the drive's stabilization moments and cause large stabilization errors. Such asymmetry is modeled as a rotational moment created by the cross product of gravitational mass imbalance force and a rotational vector.

Imbalance moment

Figure 4.8: Elevation system - complete block diagram

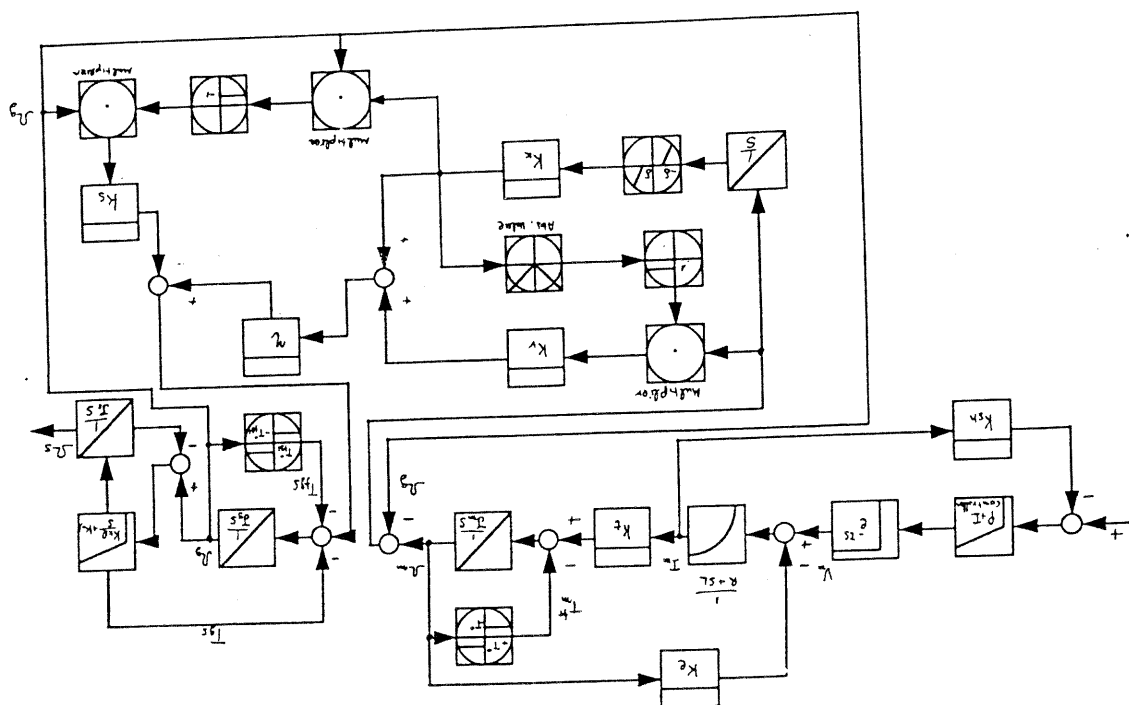
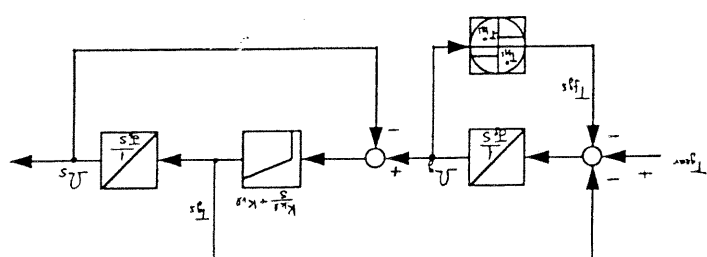


Figure 4.7: Breach block and gun barrel - block diagram



(30)

$$\frac{j_m(s) + j_m^*(s)}{j_m(s) - j_m^*(s)} = \frac{j_m(s)}{j_m^*(s)}$$

(29)

$$\frac{j_m^* + j_m}{j_m^* - j_m} = \frac{j_m}{j_m^*}$$

(28)

$$\frac{1 + \frac{K_m}{K_m * s + j_m^* s^2}}{1 + \frac{K_m}{K_m * s + j_m s^2}} = \frac{j_m(s) = (j_m^* + j_m)s}{(j_m^* - j_m)s^2}$$

Where:

(27)

$$\frac{Q_m(s)}{I_m(s)} = \frac{(j_m(s) + j_m^*)s}{1 + \frac{K_m}{K_m * s + j_m^* s^2}}$$

(26)

$$\frac{Q_m(s)}{I_m(s)} = \frac{(j_m(s) + j_m^*)s}{1 + \frac{K_m}{K_m * s + j_m s^2}}$$

follows:

Linearization of eq. (2-25) yields the transfer function of current command to motor velocity ( $Q_m / I_m$ ), and of current command to gyro velocity ( $Q_m / I_m$ ) given as

### Transfer functions

The dynamic system models described above, enable to extract useful mathematical relations. Such relations are effective tools for selecting the values of the system parameters, as follows.

## 4.2.5. DRIVES AND LOADS TRANSFER FUNCTIONS ANALYSIS

$\omega_p = \sqrt{\frac{k_s(0)}{K}}$  limits the frequency band width of the command's torque for moving the gun. The resonate natural frequency  $\omega_p = \sqrt{\frac{j_s(0)}{K}}$  may

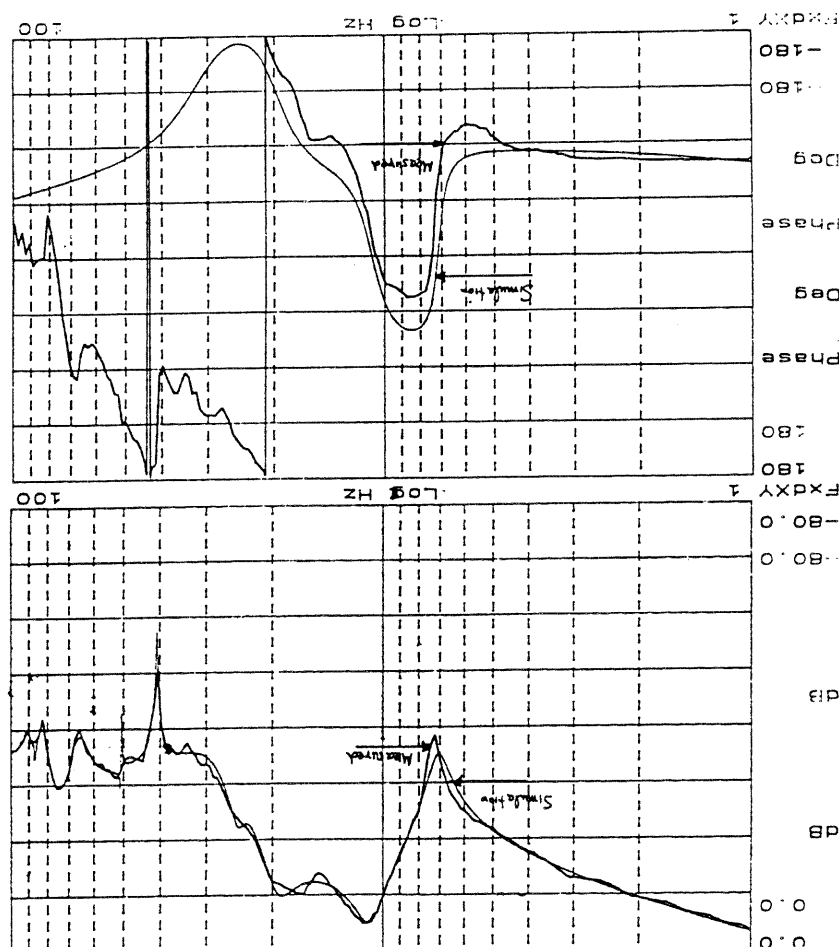
Eq. (26) yields two complex poles and zeroes which represent the gear resonance as depicted in fig (4.9). Generally, the gun resonance frequencies (given in eq 28), are located far away from the gear. For this reason, gun resonance frequency and the natural frequency are discussed separately.

## Parameters of gear and load natural frequencies

Clearly, the dynamics measured by the tachometer is quite different from the one measured by the gyro. This fact is discussed in chapter 5.

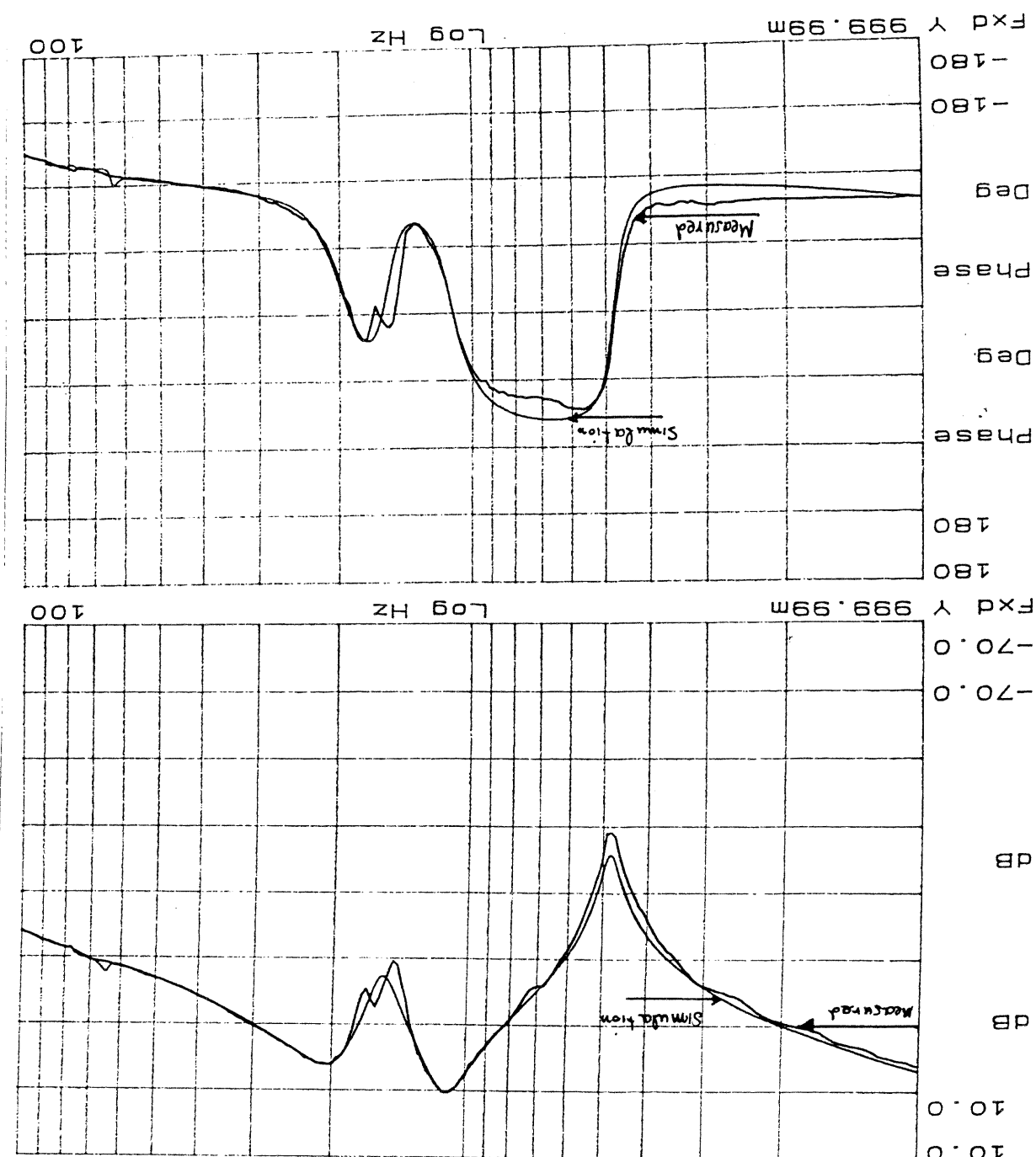
It is found that by a proper estimation of the transfer function coefficients in eq. (26-30), an exact match between the measured results to the analytic results can be achieved as depicted in fig (4.9). It can be seen that tachometer (motor velocity) output shows good agreement with all frequencies, while agreement with the gyro is good for frequencies below 30Hz.

Figure 4.9a: Gyro output versus current command - measured and simulated



Eq(28) yields the gun anti-resonance frequency namely  $\omega_g = \sqrt{\frac{J_g}{K_g}}$  and the resonance frequency namely  $\omega_r = \sqrt{\frac{J_r}{K_r}}$ . Such frequencies, observed in fig( ) enable the estimation of  $K_g$ ,  $K_r$ ,  $J_g$  and  $J_r$ .

Figure 4.9a: Tachometer output versus current command - measured and simulated



$\Theta^g(s)$  - is the gun inertial angular position.

Where:

$$\Theta^g(s) = \Omega^d(s) \frac{B(s) * K^1 * s}{1 + T_d(s) * B(s) * K^1 * s} \quad (32)$$

1. Approximation of E. (31) for low frequencies yields:

the selection of the following system parameters:  
 achieved by  
 it is observed, that minimization of the gun angular velocity can be  
 $B(s)$  - is the stabilizer transfer function.

Where:

$$\Omega^d(s) = P778 \frac{1 + J^m_s + B(s) * K^1 + J^m_s * s^2 + B(s) * K^1 * s^2 + J^m_s * K^1 * s^2}{T_d(s) * (1 + J^m_s * K^1 * s^2)} \quad (34)$$

The linear attenuation transmission function of the inertial gun angular velocity and ground disturbances, is given as follows:

Attenuation function

It can be seen that high inertia of the load, increases the attenuation of ground disturbances. This fact is helpful in view of the negligible effect of the controller in high frequencies.

$\Theta_a(s)$  is the angular position ground disturbance.

Where:

$$\Theta_a(s) = \frac{s + j_m^a(s)}{\Theta_a(s)K_a + T_a(s)} \quad (34)$$

3. Approximation of Eq. (15) with high frequencies yields:

It can be observed that selections of  $(\frac{j_m}{j_s + j_m})$  contribute to the attenuation of ground disturbances. It is recommended to select  $j_m < 0.15 * (j_s + j_m)$ , which means a lower drive moment of inertia.

$$\Omega_a(s) = \frac{1 + \frac{j_m s}{j_s(s) + B(s) * K_a}}{\frac{j_m s}{j_s(s) + B(s) * K_a} + \frac{j_m}{T_a(s)}} \quad (33)$$

2. For higher frequencies Eq. (31) yields:

It can be realized that in a low frequency, large values of torque coefficient  $K_a$ , and of stabilization  $B(s)$  can minimize inertial gun integration part of the controller can eliminate the slow changes of controller (proportional and integral). In low frequencies the high gain of the integration part of the controller can minimize the velocity and torque ground disturbances.

The control of the gun is achieved by using the feedback output of a relative sensor mounted on drive axis or on the trunion axis and regulating the gun inertial position rather than the drive or trunion axes, it is convenient to locate the sensors on the gun.

In the turret instead of on the gun, the sensor is selected in a component different from the one that must be controlled. For example, Beyers [5] at all, suggested a CSB mounted environment conditions and technological difficulties, the location of mechanical component that is controlled. At times, due to extreme value and the relevant sensor output. Sensor location determines the This error is calculated by the difference between the command signal tracking error.

Sensors are the main feedback component for closing control loops. The performance of a tracking system is checked by the rate of the discussed in [11]. A brief survey of the subject is introduced. The sensor location problem and its effect on turretgun servo system is

## 5.2. THE EFFECT OF SENSOR LOCATION ON TURRET/GUN CONTROL SYSTEMS

The problem of non-linear mechanical effects on the stabilizer performance is discussed. Feed forward techniques to achieve high stabilization performance are described. Compensation control techniques for such non-linearity are described and analyzed. Direct measurements, in both the time and frequency domain, are given. Modeling and simulation results are presented.

Control techniques to cope with the sensor location effects are and a discussion of its effect on the gun servo system, is detailed. MBT stabilizer functions, are presented. The problem of sensor location in this chapter, control optimization techniques for construction of the

### 5. SERVO CONTROL OPTIMIZATION TECHNIQUES

#### 5.1. GENERAL

It is necessary to fully understand the consequences of locating the sensor that way. Two control options are available. One based on the tachometer output as a feedback and the other on the output of the elevation gun gyro. For a stationary tank, the output of the gyro is not different in principle, from that of the tachometer. When the tank is moving, the elevation tachometer output is indicative of the velocity between the hull and the turret. However, the outputs of the gun gyro represent the inertial gun velocity in elevation and traverse, of the gun axes.

It can be seen that the dynamics, measured and simulated by gyro and tachometer, are quite different, as detailed in figure 4.1. The phase of tachometer frequency response is higher than  $-90^\circ$  for all frequencies ranges. There is no problem to synthesize a simple PI (proportional and integral) high gain controller to achieve a large bandwidth of over 100Hz, without running into the danger of instability. However, the open loop response of the gyro indicates a dangerous resonance of the gun barrel at frequencies higher than 12Hz, expressed by a sharp drop of the phase to over  $-180^\circ$ . A high gain controller may bring about instabilities in the system. It can be seen that the tachometer frequency response expresses the drive's dynamics, while the gyro response expresses the drive's dynamics, in low frequencies, the drive and the gun drive measured by the tachometer, is high due to its low moment of inertia, while the gain of the gun measured by gyro, drops because of the high gun moment of inertia, limited gear drive stiffness and gun inertia, which gun measured by gyro, drops because of the gun's mass and the drive's mass.

The frequency response of the tachometer in a closed loop using high gain PI controller, is given in fig. 5.1. It can be seen that the bandwidth possible to obtain a better response to a step function if a smaller gun barrel, as measured by the gyro. See Fig. 5.2.

Clearly, the measured response to a step function is fast with only a small overshoot. However, it does not describe well the response of the gun barrel, as seen in this case.

It can be seen that the latter is quite resonant. On the other hand it is possible to obtain a better response to a step function if a smaller bandwidth controller is carefully selected, taking into consideration the response of the gun bar. Figures 5.3, 5.4 show a much smoother response in this case.

It can be concluded that due to the difference between gun dynamics and drive dynamics, the gun stabilizer must be driven by the signals of inertial sensors, located on the gun.

The gyro closed loop frequency and time response depicted in fig. 5.6 and fig. 5.7 respectively, indicates that a bandwidth of 4Hz is achieved without getting into resonant condition as result of a step input.

The information given in eqs. (31, 35) and in figure (5.5) yields the structure and control requirements on the stabilizer function  $B(s)$ .

$$Io(\Theta_{stab}) = \sqrt{\int_{\omega_1}^{\omega_2} PSD(\Theta_{stab}) d\omega} = \sqrt{\left( \int_{\omega_1}^{\omega_2} PSD(\omega_i) \right)} \leq 0.4 \text{mm} \quad (35)$$

The gun resonances measured by the gyro can be attenuated by using suitable notch filters. Such attenuation allows the use of a high gain PI controller. The construction of the stabilizer functions is based on the ground disturbance's Power Spectrum Density (PSD) and on the required attenuation function. In figure 5.5, a measured PSD of ground disturbances is shown. Eq. (31) yields the inertial gun velocity inaccuracy caused by ground disturbances. The required gun position stabilizer accuracy yields:

**Figure 5.1: Step response of tachometer loop with high gain PI**

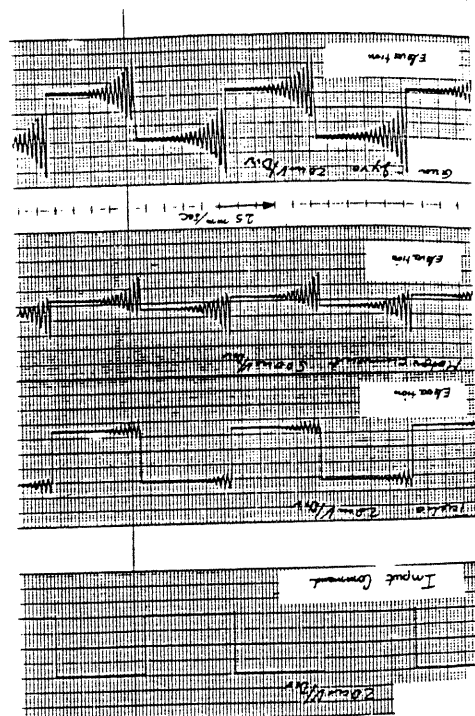


**Figure 5.1: Bode diagram of tachometer loop with high gain PI**

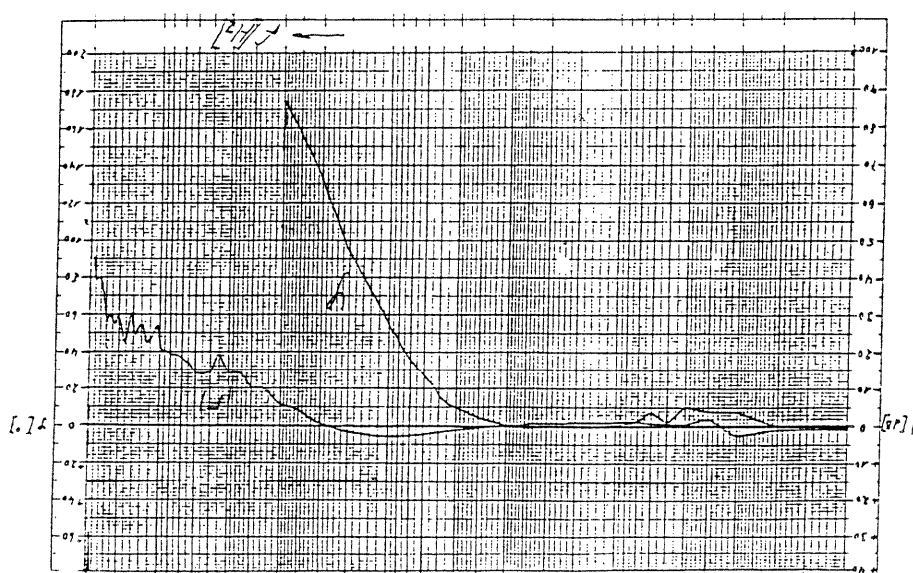


Figure 5.1: Step response of tachometer loop with PI controller -  
as measured

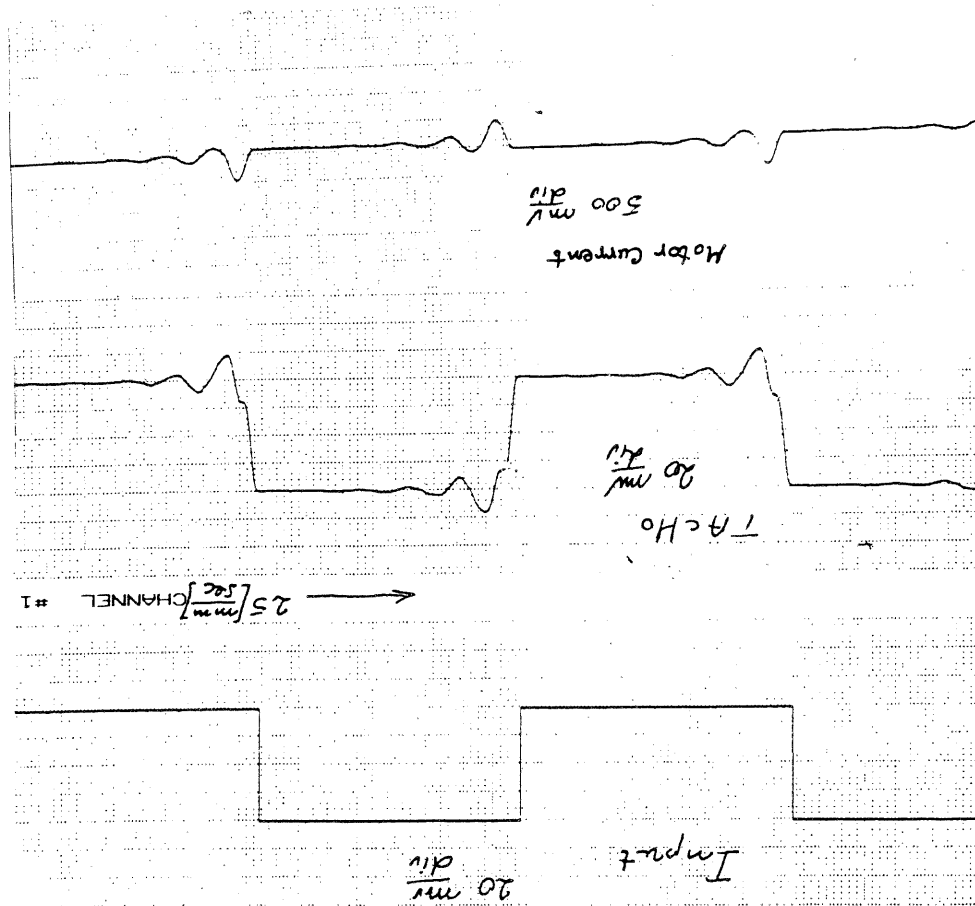


Figure 5.1: Bode diagram of tachometer loop with PI controller -  
as measured

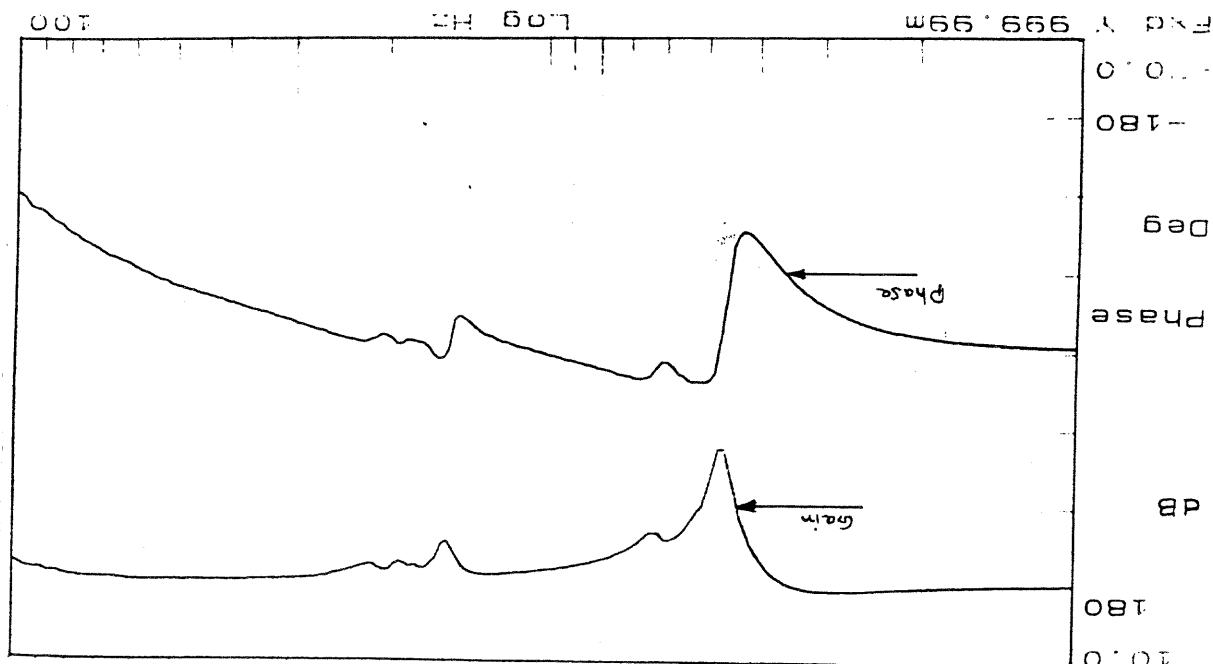


Figure 5.6: Bode diagram of gyro close loop - as measured

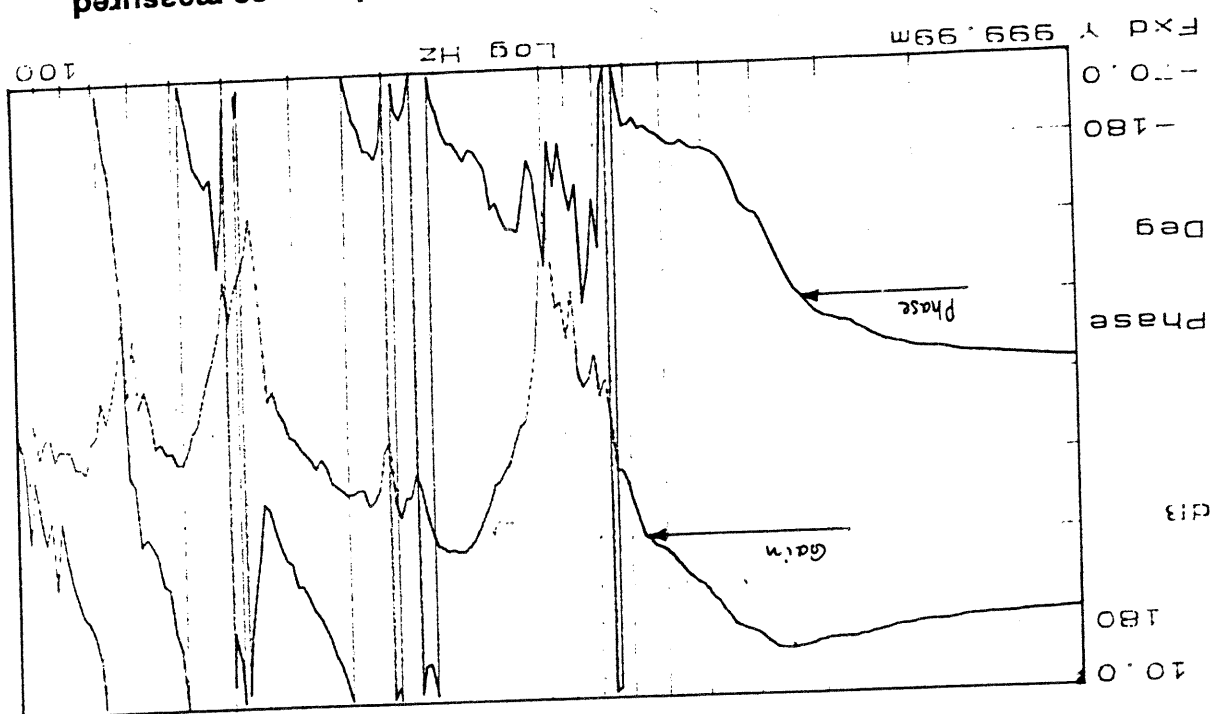


Figure 5.5: PSD of velocity disturbances

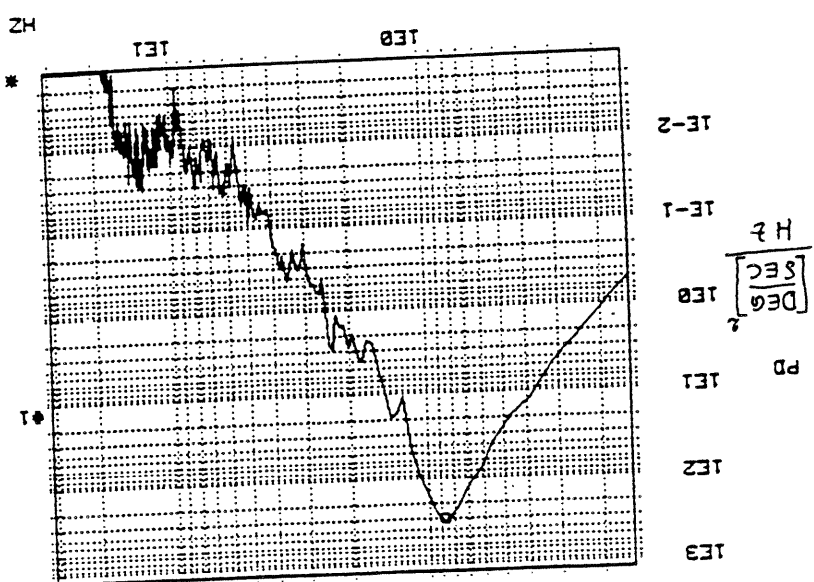
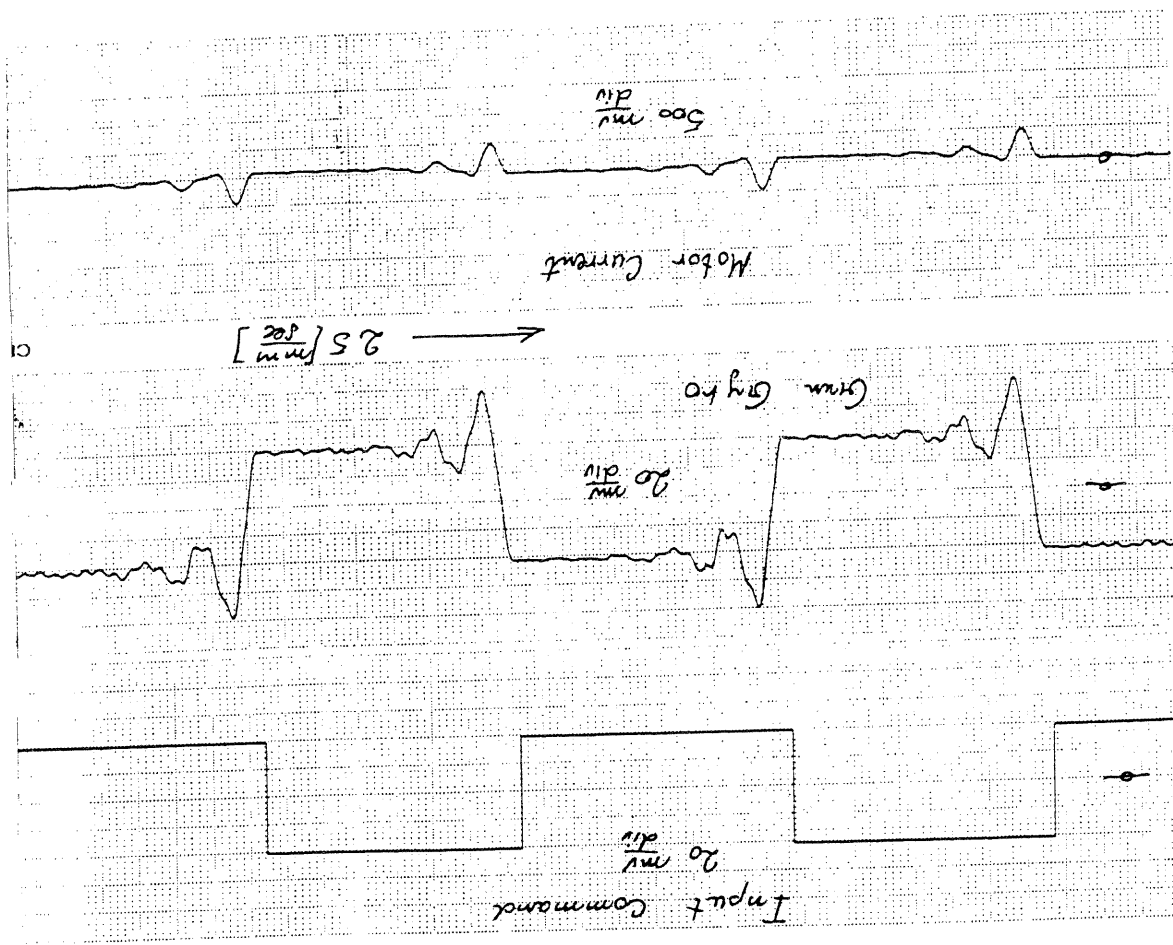


Figure 5.6: Step response of gyro close loop - as measured



### 5.3.

#### COMPENSATION TECHNIQUES FOR SYSTEM FRICTION

##### BACKLASH COMPENSATION

- The two main mechanical system non linearities are the backlash and friction. The problem of backlash compensation is difficult and is not completely solved yet. Recently, theoretical adaptive control strategies [13] for backlash compensation are given. The basic idea for backlash compensation is to employ:
- an inverse backlash model
  - an adaptive backlash parameter estimator.

With such information, feed forward signals for compensation of backlash can be computed in real time. Simulation results reveal good performance. However, there are no reports yet on practical results. On the basis of our experience, it is recommended to build the drives such that the backlash will be smaller than  $±0.05\text{mm/radiam}$ .

$$I_{\text{anti-friction}} = \left( \frac{K}{T_0} \right) SGN(\Delta_{\text{current-command}}) \quad (36)$$

The result is injected as a feed forward negative moment to the current loop. It is found that with such technique, a major improvement is achieved in the performance of the aiming function. The anti-friction loop is implemented function used in this case, is of the following form:

By such a technique, the friction effects are diminished. This technique is similar to the control principle of "inverse dynamics" and "computed torque", applied extensively for robots [14]. As mentioned above, friction moments affect the aiming minimal slew rate and the velocity command is employed for the compensation of the inverse friction effects on the aiming function is detailed. The gunner aiming stabilisation accuracy. In fig 5.8, the principle of compensation of friction moments is illustrated. As mentioned above, friction moments affect the aiming minimal slew rate and the dynamic of system's coulomb friction moment.

Friction effect minimum velocity compensation is implemented by applying the principle of "inverse dynamics" and "computed torque". With such control strategy, an inherently suitable friction model is included in the MBT stabilizer to predict and to compensate for the friction. The compensation is achieved by computing the predicted friction moment with negative sign and injecting it as a feed forward in the drive's current loop.

#### Fricution effect minimum velocity compensation

Compensation of the friction effects is feasible scheme implemented by digital means [14].

The idea of compensation of velocity disturbances is based on direct measurements of velocities, computing the results in the current control loop. In disturbances and injecting the results in the current control loop. In traverse, a feed forward gyro, mounted on the hull, measures the elevation ground velocity with the gun elevation stabilization. In elevation, a feed forward gyro is mounted on the turret and measures disturbances and injecting the results in the current control loop. In traverse, a feed forward gyro, mounted on the hull, measures the elevation ground velocity with the gun elevation stabilization. In

achieved by using feed forward techniques. It is found that due to bandwidth limitation of the conventional servo control loops and system non linearity, limited stabilization accuracy is achieved. However, a major stabilization performance improvement is achieved.

Ground disturbances acting on an MBT on the move, comprise velocity imbalance and MBT accelerations. Disturbances and moment disturbances, created by gun/turret

#### 5.4. GROUND DISTURBANCES COMPENSATION TECHNIQUES

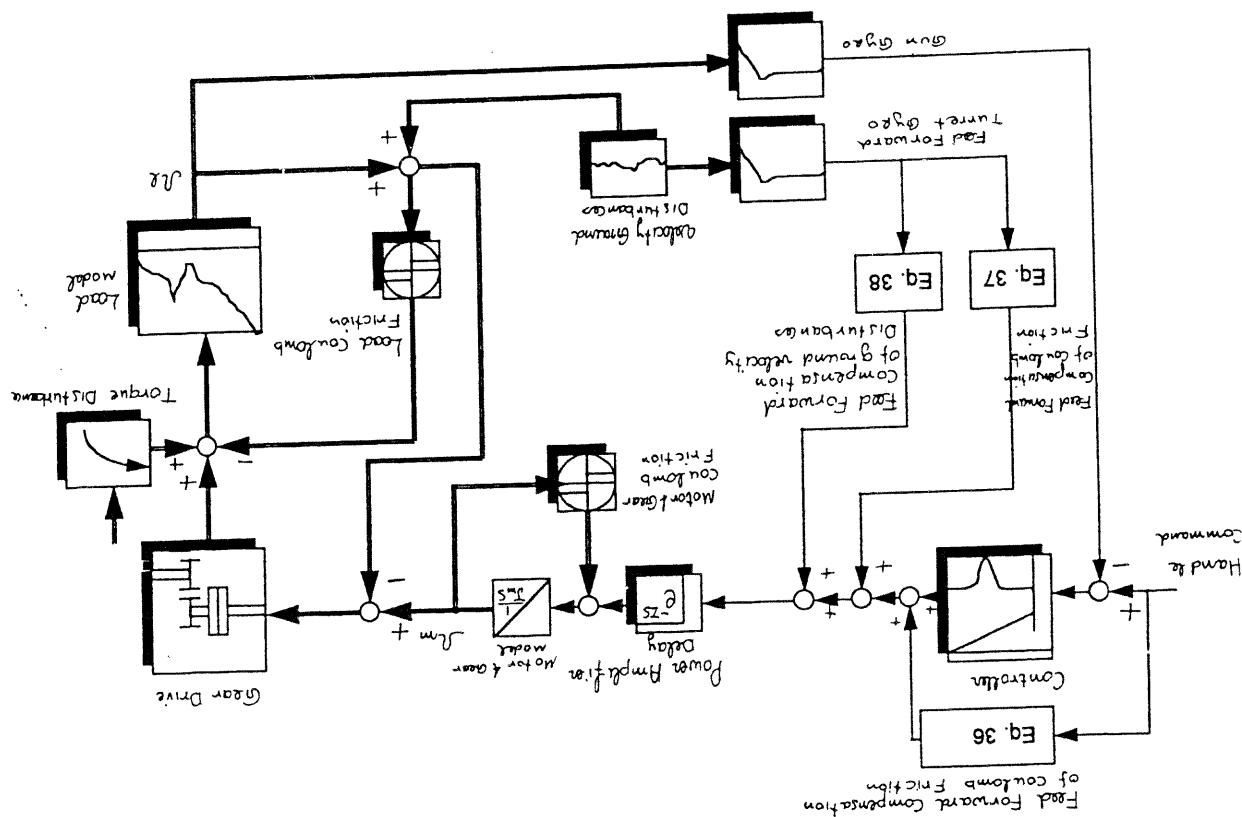
Such velocities are sampled to compute the system friction moment dynamics. The results are injected as feed forward to current loops for major improvement of gun stabilization accuracy is achieved. The friction simplified compensation function for ground velocity diminishes the friction moment disturbances. With such a technique, a friction disturbances has the form of:

$$I_{\text{friction}} = \left( \frac{K}{T_0} \right) SGN(\alpha_{\text{ground-disturbance}}) \quad (37)$$

The compensation is based on the velocity of the ground disturbances, compensation of friction effects on the stabilization accuracy is detailed. Can minimize such degradation. In figure 5.8, the principle of it is recognized that Coulomb friction degrades also the stabilization accuracy. However, our research yields that the anti friction technique can minimize such degradation. In figure 5.8, the principle of

##### Friction effect on stabilization accuracy compensation

Figure 5.8: Compensation techniques for ground and mechanical disturbances

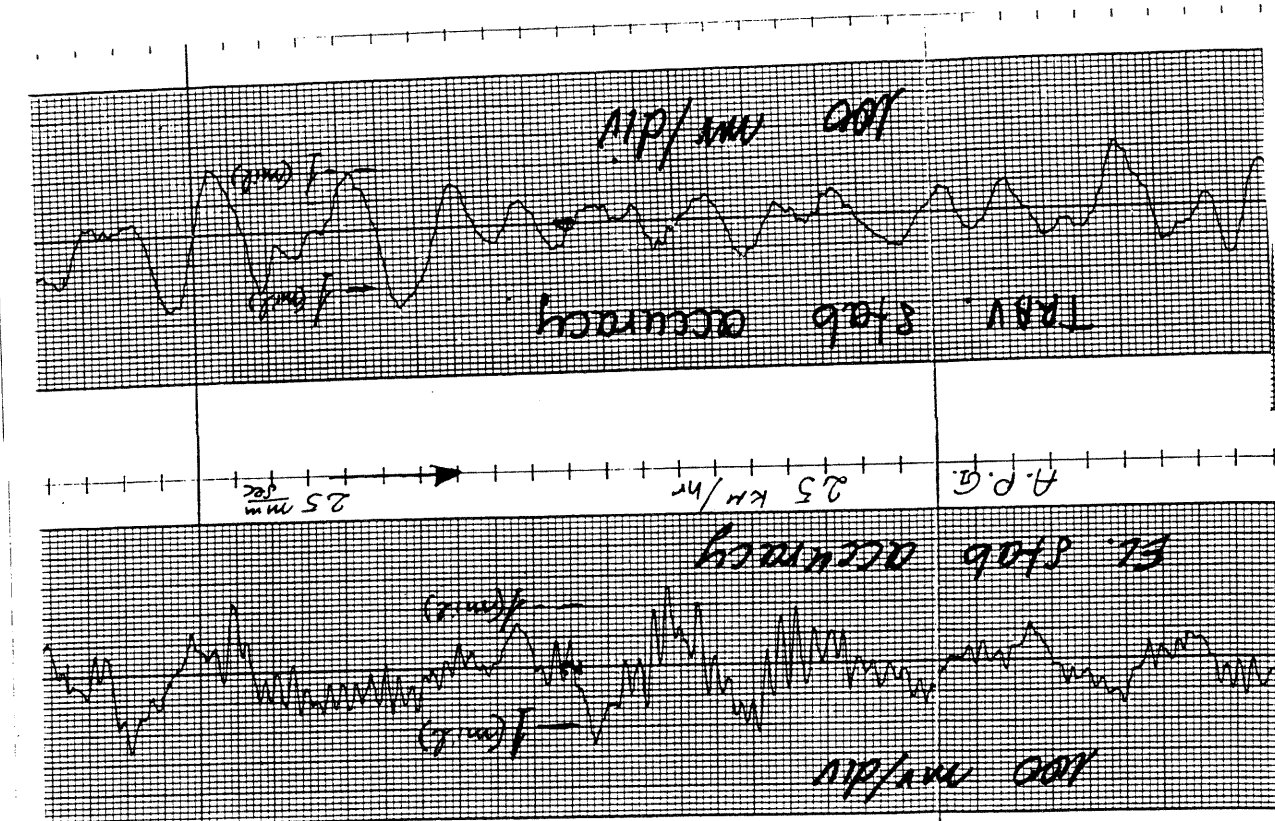


The compensation of dynamic imbalance moments can be realized by using accelerometers on the gun. The output of which is employed to compute the instantaneous imbalance moments. The results are combined with the servo control loops as feed forwards. In figure (5.8), a schematic description for the feed forward techniques described above, is given.

$$I_{\text{ground-disturbance}} = J_m * K_{\text{drive}} \left( \frac{d\alpha}{dt} \right) \quad (38)$$

It can be shown that the simplified, computed transfer function of the feed forward is of the form:

**Figure 5.9:** Gun stabilization without Feed Forward compensation



sigma.

After integrating the above mentioned compensation techniques, much better results are achieved, as detailed in figure (5.10). It is found that the achieved stabilization accuracy is better than 0.2 milliradian one

In figure (5.9), the gun stabilization accuracy in elevation in an APG course is detailed, without the use of any feed forward compensation techniques. The calculated stabilization accuracy is 0.5 milliradian one sigma. The maximum ground disturbance velocity is about 30deg/sec. The influence of the gun friction can be observed by the square wave type of the gun position signal. Note that the velocity of the MBT is 25km/hr. This result is achieved only with the aide of the rate integrating gyros mounted on the gun.

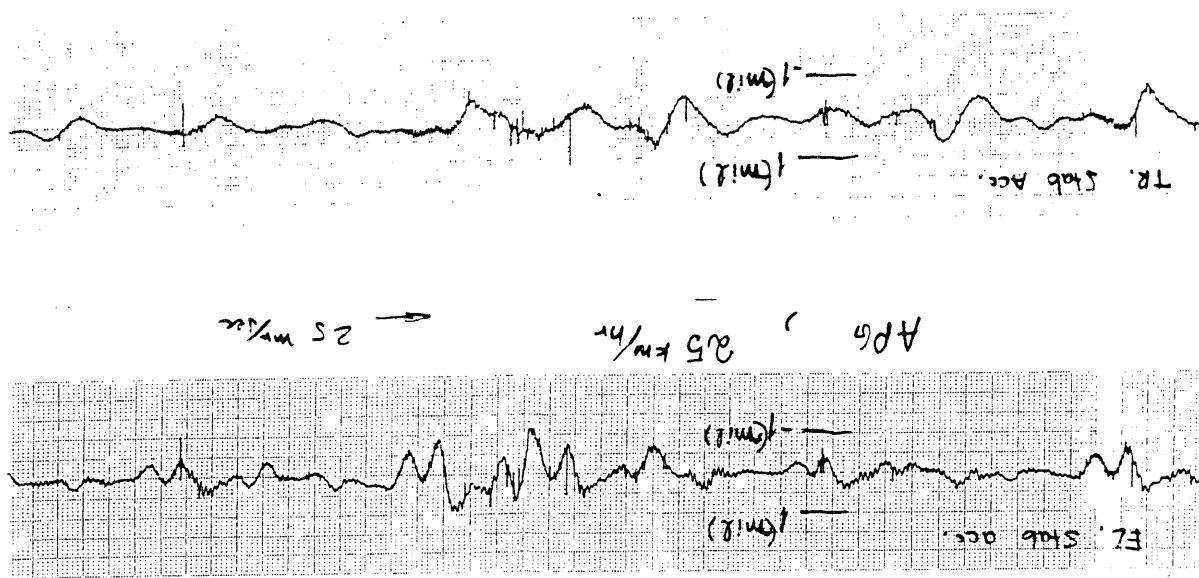
In this chapter, results of field test stabilization accuracy of an MBT are described. The stabilized gun position is measured by the integration of the gun elevation gyro output.

## 5.5. STABILIZATION RESULTS

In this paper, selected topics on the synthesis, analysis and design of an all electric drive system for an MBT are described. Basic structures of such drives are given. Analysis of customers' requirements using mathematical models, yields a methodology for the construction of such systems. The effects of sensor location on the control system are analyzed. It is found that, for inertial gun stabilization purposes, it is convenient to use inertial sensors on the gun rather than relative sensors on drive's axis. This, due to the different dynamics of the controlled components. Sophisticated feed forwards for achieving high stabilization performance are described in detail. Stabilization performance and field results are described, revealing the effectiveness of the proposed techniques.

CONCLUDING REMARKS 6.

Figure 5.9: Gun stabilization with Feed Forward compensation



1. Chryslar Corporation, "A Mathematical Representation of The M60A1 Azimuth and Elevation Control and Add-On Stabilization System", Nov. 1971.
2. Ogorokiewicz, R.M., "Stabilized Tank Gun Controls", International defense review, vol. 5, 1978, pp. 725-728.
3. Wolfgang Schneidler, "Gunnerry With the Soviet T-72/M1 Tank", International Review, vol. 1991, pp. 491-494.
4. Hammig, M., "Lecerc", International Defense Review, Vol. 9, 1990.
5. Beyer, O. and B. Kirszt, "Method and Apparatus for Stabilizing High-Dynamics Devices", United States Patent, Patent Number 4,924,749, May 15, 1990.
6. Scheib, H.J., "Ein adaptiver Ljapunow-Regler fur Riccati - und Stabilisierungs", Karlsruhe, Automatisierungstechnik at, 33, Jahrgang, Heft 12/1985, pp. 365-372.
7. Electro-Craft Corp., "DC Motors Speed Controls Servo Systems", An Engineering Handbook, Aug, 1980.
8. Kittlich, M., "Uber die Nachbildung von Getrieben auf dem Analogrechner", Electronica Rechenaal, 8(1966), H.3, S. 125-130.
9. Dahl, P., "A Solid Friction Model. Technical Report TOR-0158(3107-18)-1, The Aerospace Corporation, El Segundo, CA, 1968.

## LITERATURE

10. Chubb, B.A., "Modern Analytical Design of Instrument Servomechanisms", Addison-Wesley Publishing Company, 1967.
11. Davidov, G. and A. Shavit, "The Effect of Sensor Location On the Control of TurretGun Systems", The Israel Conference on Mechanical Engineering, May 1992.
12. Warath, P., "Adaptive Bearing Compensation Based on Recent Knowledge of Dynamic Friction", Automatica, 20(6):717-727, 1984.
13. Tao, G. and P.V. Kokotovic, "Adaptive Control of Systems with Unknown Output Backlash", Trans. on Aut. Contr., Feb. 95, Vol. 40, No. 2, pp. 326-330.
14. J.Y.S. Luh, M.W. Wallen and R.P.C. Paul, "Resolved Acceleration control of mechanical manipulators", IEEE Tr. on Aut. Contr., Vol. AC-25, No. 3, 1980.